Modelling Damage and Stochastic Properties in Engineering Structures

Olsson, Anders

1999

Document Version:
Publisher's PDF, also known as Version of record

LUND UNIVERSITY

MODELLING DAMAGE AND STOCHASTIC PROPERTIES IN ENGINEERING STRUCTURES

ANDERS OLSSON

Department of Mechanics and Materials

Structural Mechanics

Licentiate Dissertation

Department of Mechanics and Materials
Structural Mechanics

ISRN LUTVDG/TVSM--99/3037--SE (1-80)
ISSN 0281-6679

MODELLING DAMAGE AND STOCHASTIC PROPERTIES IN ENGINEERING STRUCTURES

ANDERS OLSSON

Printed by Universitetstryckeriet, Lund, Sweden, 1999.

For information, address:
Division of Structural Mechanics, LTH, Lund University, Box 118, SE-221 00 Lund, Sweden.
Homepage: http://www.byggmek.lth.se

Preface

The research presented in this licentiate thesis has been carried out at the Division of Structural Mechanics, Lund Institute of Technology. The first part of the work, concerning the safety of pallet racks in industry, was financed by the Swedish Council for Work Life Research, whose support is gratefully acknowledged.

I would like to express my gratitude to my supervisor, Professor Göran Sandberg, for his guidance, support, and encouragement during this work. Special thanks also to Bo Zadig, for his skillful drawing of the more complicated figures, and to my room neighbour, Erik Serrano, for always being willing to advise me and help me with everyday matters such as the handling of computer software. I would also like to thank all my other friends and colleagues at Structural Mechanics for help and inspiration.

Several people outside the Division of Structural Mechanics have been very important to the present research. Special thanks to Krystoffer Mroz, formerly employed at the Swedish National Testing and Research Institute, and Karl-Gustav Carlsson, Constructor Sweden AB, who were the project leader and the industry representative respectively of the project financed by the Swedish Council for Work Life Research. Furthermore, I am grateful to Professor Jacques de Maré, Mathematical Statistics, Chalmers University of Technology, for giving me valuable comments, from a mathematical statisticians point of view, on the manuscript of the third paper in this licentiate thesis.

Finally, I wish to express my gratitude to my wife, Martha, for all her love and support during the course of this work.

Lund, September 1999

Anders Olsson

Contents

Summary of papers 1–3

Paper 1 The influence of damage on the load-carrying capacity of thin-walled steel columns with channel sections is investigated. The axial load-carrying capacity is evaluated for different profiles, and different damage magnitudes are dealt with. The profiles selected for the analysis are commonly used as upright elements in rack and shelving systems in industry. The type of damage corresponds primarily to truck impacts. The strategy presented, however, is generally applicable to different types of profiles, and suitable for parameter studies of different types of damage, load cases, and boundary conditions. The main part of the analysis consists of numerical simulations using the finite element method, but a verifying laboratory test series is also presented. The results of the numerical simulations are in good agreement with the laboratory tests, and show that even very small defects in the thin-walled columns significantly reduce the axial load-carrying capacity.

Paper 2 The paper suggests a method to consider uncertainties in engineering structures in a computational scheme. Latin hypercube sampling is used to prepare input data of probabilistic parameters for subsequent deterministic simulations, in which the mechanical response is evaluated. The approach is applied on a pallet rack system where damaged columns and connector stiffnesses are considered as probabilistic parameters. The mechanical simulations are performed with the finite element method, and full advantage is taken of existing commercial code.

Paper 3 The paper suggests a Latin hypercube sampling method, with correlation control, for stochastic finite element analysis. This sampling procedure significantly improves the representation of stochastic design parameters compared to standard Monte Carlo sampling. As the correlation control requires the number of realizations to be larger than the number of stochastic variables in the problem, principal component analysis is employed to reduce the number of stochastic variables. In many cases this considerably relaxes the restriction on the number of realizations. Furthermore, it is an advantage to combine the sampling method with the well-known Neumann series expansion method for solving the equation systems efficiently. The paper comprises an extensive comparison of different sampling methods and perturbation methods for stochastic finite element analysis. It is shown that the Latin hypercube sampling plan, with correlation control, in conjunction with the Neumann series expansion method, is a competitive approach regarding computational efficiency as well as general applicability.

Introduction

Background

The theory and methods of computational mechanics have developed significantly during the last decades, and become widespread in engineering design practice through extensive commercial computer software usage. In most design cases, however, the engineer is left with uncertainties about how to actually model a structure. The uncertainties can be directed towards the strength, stiffness, or geometrical properties of structural elements or connections. Production errors or damage caused by accidents or inadequate management are in many civil engineering structures uncertain parameters which should be considered in the analysis as well. Other issues are how the load is applied and, in dynamic analysis, the time history of the load. Two concrete examples containing obvious uncertainties are the stochastic loading from traffic, wind, and waves on bridges, and the strength and stiffness of connectors of temporary structures such as scaffoldings at building sites that are exposed to wear as they are repeatedly assembled and taken apart. Other examples, connected with ongoing research projects at the Division of Structural Mechanics, are the random structure of cellulose fibre materials (Heyden 1996), and the strength of finger-joints for laminated wooden beams (Serrano 1997).

There is a growing realization that unavoidable uncertainties must be considered in a computational scheme to produce reliable computational and engineering results. Traditionally, designers have used safety factors to provide increased confidence in the structural performance, but this approach is insufficient in obtaining information about the distribution of the response parameters, especially for large and complex systems. This has lead to a rather extensive research aiming at combining efficient methods of structural analysis with stochastic analysis in which the influence of random variables is evaluated. The only method that has become widespread in engineering design practice is the Monte Carlo simulation technique. Probabilistic design parameters are sampled and a number of deterministic calculations are performed to provide information about the distribution, or some statistics of response parameters. This is an accurate and simple approach, but also very expensive in terms of computer resources. Several methods that could be employed at a lower computational cost have been proposed. These can be divided into three main categories. The methods of the first category concern the sampling itself of the Monte Carlo technique in order to reduce the number of realizations

required to provide reliable statistics of the response. Stratified sampling and Latin hypercube sampling belong to this category. Most work in this area has been carried out by mathematical statisticians [e.g. McKay et al. (1979); Iman and Conover (1982); Kjell (1995)], and elaborate sampling techniques are rarely employed in the field of structural analysis using finite elements. A major advantage of these methods is that the consequent analyses, i.e. the runs determined by the sample, are identical to the deterministic analysis. Thus, full advantage can be taken of existing commercial codes developed for deterministic analysis (Sandberg et al. 1997).

The methods of the second category also employ Monte Carlo simulations. However, the strategy is to reduce the computational work by using efficient solution techniques for the equation system of each run by making use of the similarity between the different realizations. The Neumann series expansion method, and the preconditioned conjugate gradient method belong to this category. The Neumann series expansion method in conjunction with the standard Monte Carlo technique has been employed by several researchers and found to be efficient [e.g. Yamazaki et al. (1988); Chakraborty and Dey (1996)]. The preconditioned conjugate gradient method has been used in conjunction with the Neumann series expansion method, and the standard Monte Carlo technique by Papadrakakis and Papadopoulos (1996).

Methods of the third category do not compute the response statistics through Monte Carlo simulations but through series expansions of random variables. The most well-known methods are probably: the Taylor series expansion method, in which a truncated Taylor series of the response variable is established (Liu et al. 1986; Kleiber and Hien 1992), the Neumann series expansion method, in which a truncated Neumann series is employed for the equation system (Shinozuka and Deodatis 1988; Spanos and Ghanem 1989), and the basis random variable method, in which the statistics of the response variables are evaluated by minimizing the potential energy of the system with respect to statistics of the basis random variables (Lawrence 1987). A comprehensive exposition of a wide range of stochastic finite element methods, from the second and third category, is given in Matthies et al. (1997).

Purpose and scope of the present work

The purpose of the present work is to suggest and compare strategies and methods for calculating the influence of stochastic properties in engineering structures. Importance is attached to general applicability as well as to computational efficiency, and the research is, to a great extent, performed in close connection with realistic target applications.

This licentiate thesis contains three papers. The first two focus on a typical engineering application, namely the uncertain properties of pallet racks used in industry. One such property is the loading. Naturally, the loading varies with time as the need for storage is different from one time to another. Some industries might need to store large quantities of goods before the peak season, or before a large shipping of a certain product. This is not very remarkable, and it does not cause risky situations by itself as the pallet racks are designed for maximum loading. However, in combination with rebuilding and changes in the geometry of the pallet rack not taken into account in the design, dangerous situations might appear. Even worse, if structural elements and connectors are damaged or removed, as they quite often are as a result of accidents or inadequate management, there is a significant risk of failure and severe accidents might occur. In the present papers the influence of truck impacts to thin-walled columns is thoroughly evaluated. What is the influence of such damage with respect to the load-carrying capacity of the system? Naturally, this depends on the number of impacts, the extent of the impacts, the positions of the impacts, and the type of profile used. The first paper concerns the influence of damage to individual thin-walled steel columns. The study comprises numerical simulations as well as laboratory tests. Different impact directions and damage levels are investigated and the reduction in axial load-carrying capacity is evaluated. The results of the first paper constitute input to the second paper where the extent and positions of the impacts are regarded as stochastic parameters. The reduction of the global load-carrying capacity due to damage is calculated. The second paper also comprises a study of the influence of uncertainty in the stiffness of the beam-end connectors. Fig. 1 shows a typical pallet rack used in industry. Damaged columns and floor connectors are highlighted as well as a beam-end connector. Additional parameter studies on pallet racks, especially concerning changes in geometry, and removal of structural elements, are found in Olsson and Sandberg (1998).

As stated above, suitable statistical methods are needed for this type of analysis. In the third paper of this licentiate thesis several statistical methods are described, and compared with respect to computational efficiency and general applicability. One of the methods examined, the Latin hypercube sampling plan for Monte Carlo simulations, is found to possess excellent qualities in both these respects. Unfortunately, however, in order to control the correlation of the input variables efficiently, the method requires that the number of realizations, corresponding to deterministic runs, exceeds the number of stochastic variables in the problem. This is a severe restriction in many structural mechanics applications. However, in this paper a further development of the Latin hypercube sampling plan is suggested, which relaxes the restriction of the number of runs vs. the the number of stochastic variables and brings the method into line with finite element analysis.

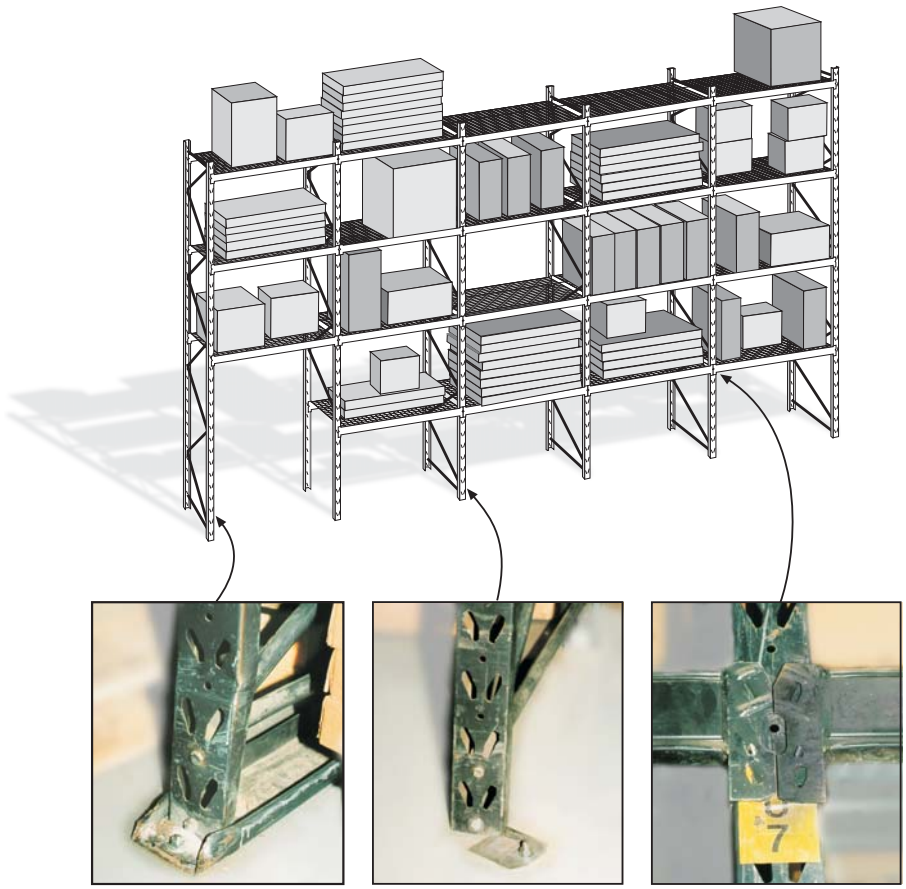

Fig. 1. *A typical pallet rack used in industry. Damaged columns and floor connectors are highlighted, as well as a beam-end connector.*

References

Chakraborty, S., and Dey, S. S. (1996), "Stochastic finite element simulation of random structure on uncertain foundation under random loading." *Int. J. Mech. Sci.*, **38**, 1209–1218.

Heyden, S. (1996), "A network model applied to cellulose fibre materials." *Rep. TVSM-3018,* Lund Inst. of Techn., Div. of Struct. Mech., Lund, Sweden.

Iman, R. L., and Conover, W. J. (1982), "A distribution-free approach to inducing rank correlation among input variables." *Communications in Statistics - Simulation and Computation*, **11**, 311–334.

Kjell G. (1995), "Computer experiments with application to earthquake engineering." *Rep. 1995:7, Studies in Statistical Quality Control and Reliability,* Chalmers Univ. of Techn., Dep. of Math. Stat., Gothenburg, Sweden.

Kleiber, M., and Hien, T. D. (1992), "The Stochastic Finite Element Method." *Wiley*, Chichester, England.

Lawrence, M. A. (1987), "Basis random variables in finite element analysis." *Int. J. Num. Meth. Engrg.*, **24**, 1849–1863.

Liu, W. K., Belytschko, T., and Mani, A. (1986), "Random field finite elements." *Int. J. Num. Meth. Engrg.*, **23**, 1831–1845.

Matthies, H. G., Brenner, C. E., Bucher, C. G., and Soares, C. G. (1997) "Uncertainties in probabilistic numerical analysis of structures and solids – stochastic finite elements." *Structural Safety*, **19**, 283–336.

McKay, M. D., Conover, W. J., and Beckman R. J. (1979), "A comparison of three methods for selecting values of input variables in the analysis of output from a computer code." *Technometrics*, **21**, 239–245.

Olsson, A., and Sandberg, G. (1998), "Parameter studies on pallet racks." *Rep. TVSM-7122,* Lund Inst. of Techn., Div. of Struct. Mech., Lund, Sweden.

Papadrakakis, M., and Papadopoulos, V. (1996), "Robust and efficient methods for stochastic finite element analysis using Monte Carlo simulation." *Comput. Methods Appl. Mech. Engrg.*, **134**, 325–340.

Sandberg, G., Kjell, G., and de Maré, J. (1997), "Computational planning using Latin hypercube sampling." *Report TVSM–7118*, Lund Inst. of Techn., Div. of Struct. Mech., Lund, Sweden.

Serrano, E. (1997), "Finger-joints for laminated beams - experimental and numerical studies of mechanical behaviour." *Rep. TVSM-3021,* Lund Inst. of Techn., Div. of Struct. Mech., Lund, Sweden.

Shinozuka, M., and Deodatis, G. (1988), "Response variability of stochastic finite element systems." *J. Engrg. Mech.*, **114**, 499–519.

Spanos, P. D. and Ghanem, R. (1989), "Stochastic finite element expansion for random media." *J. Engrg. Mech.*, **115**, 1035–1053.

Yamazaki, F., Shinozuka, M., and Dasgupta, G. (1988), "Neumann expansion for stochastic finite element analysis." *J. Engrg. Mech.*, **114**, 1335–1354.

Paper 1

Load-Carrying Capacity of Damaged Steel Columns with Channel Sections

Anders Olsson, Göran Sandberg
and Per-Erik Austrell
Division of Structural Mechanics
Lund Institute of Technology

Load-Carrying Capacity of Damaged Steel Columns with Channel Sections

Anders Olsson, Göran Sandberg and Per-Erik Austrell

Division of Structural Mechanics, Lund Institute of Technology, Lund University, P.O. Box 118, SE-221 00 Lund, Sweden

Abstract

The influence of damage on the load-carrying capacity of thin-walled steel columns with channel sections is investigated. The axial load-carrying capacity is evaluated for different profiles, and different damage magnitudes are dealt with. The profiles selected for the analysis are commonly used as upright members in rack and shelving systems in industry. The type of damage corresponds primarily to truck impacts. The strategy presented, however, is generally applicable to different types of profiles, and suitable for parameter studies of different types of damage, load cases, and boundary conditions. The main part of the analysis consists of numerical simulations using the finite element method, but a verifying laboratory test series is also presented. The results of the numerical simulations are in good agreement with the laboratory tests, and show that even very small defects in the thin-walled columns significantly reduce the axial load-carrying capacity.

Keywords: Thin-walled, Column, Steel, Channel section, Damage, Load-carrying capacity, Racking system, Finite element method

1 Introduction

Thin-walled steel profiles with channel sections are commonly employed in civil engineering structures to resist lateral and axial loads. The sections are easily assembled to other structural members through welding or bolting. They are inexpensive to manufacture and fabricate as they may be pressed or rolled from flat steel sheets or coiled strips. Although these profiles perform very well as structural members in relation to their weights, they are susceptible to different types of buckling including distortion of the cross section, local buckling, and torsional instability. They are also sensitive to initial imperfections and damage.

Much research has been aimed towards accurate and efficient analysis of thin-walled beam columns in terms of conventional beam theory, finite strip analysis, and finite element analysis. Conventional beam theory proceeds from the kinematic assumption that the cross section does not distort. The modes of deformation are limited to extension, bending about two principal axes and torsion. However, beam theory can be extended by also incorporating distortional modes of deformation. This approach has been employed by Davies and Leach (1992) using a generalized beam theory developed by Schardt (1989). Another method for analysis of thin-walled beam columns is the finite strip method, where the thin-walled member is subdivided into longitudinal strips. This method includes distortional modes because each strip is free to deform both in and out of its plane. Buckling of channel sections for storage racks without imperfections has been analyzed using this method by Hancock (1985). Nonlinear material models have also been incorporated. Clarke (1994) and Rasmussen and Rondal (1997) used a Ramberg Osgood model and studied the influence of material parameters on the buckling behavior.

The method used in this study employs large displacement finite element analysis, material nonlinearity, and modeling by use of shell elements. This is necessary due to the complexities involved in modeling the geometry, the boundary conditions, and the material. It is then possible to model details in the geometry such as holes or local defects. Moreover, the initial damage is modeled by indentation of a rigid surface laterally into the beam columns, causing plastic deformations. Hence, this approach is suitable when local deformations and strains at some place along the beam column must be captured in detail. The disadvantage compared to the other methods is the computational cost related to model preparation and the required number of degrees of freedom.

The purpose here is to suggest and apply a strategy for investigating the effects of damage for thin-walled steel columns. The work is comprised within a project concerning failure sensitivity of pallet racks. Upright members in such structures are usually of the type described above, and if they are damaged (for example by truck impacts or because second-hand, crooked or squeezed components are used) the load-carrying capacity is reduced and the risks of failure and accidents are increased. The scope of the present investigation is restricted to three different profiles, and the type of damage considered is related to truck impacts. The main part of the analysis consists of numerical simulations using the finite element software ABAQUS (*ABAQUS* 1996). However, a laboratory test series is also performed.

2 Profiles and modeling

The three profiles selected for this study are frequently used in rack and shelving systems. One of the profiles selected for this study has an asymmetric cross section while the other two have symmetric cross sections, one C profile and one Ω profile. Fig. 1 shows one repetitive segment of each profile with corresponding element meshes. To bring down the required number of elements some simplifications in the modeling were adopted. The asymmetric profile has impresses on its broad side along the upright axis. These were neglected in the model. Further, small circular holes, occurring in all three profiles were modeled by reductions in thickness of strips along the upright axis at the location of these holes. The simplifications were performed after comparisons with finer models, considering impresses and circular holes in detail. The comparisons showed that the simplified models were able to capture the global, linear elastic stiffness, and overall deformation modes of the columns when loaded as in the simulations below. The simplified modeling of perforation in thin-walled columns has earlier been employed, and shown to be valid, by Mroz (1995).

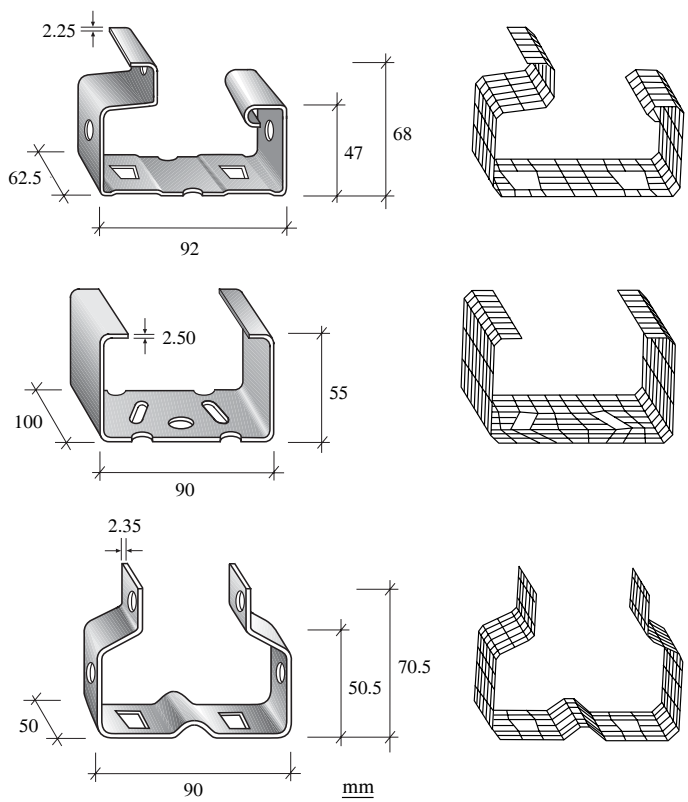

Fig. 1. *Repetitive segments of the three profiles with corresponding element meshes.*

A four-node, thin-shell element (ABAQUS element S4R5) with five degrees of freedom at each node, and reduced integration was used in the analysis. The element contains no drilling degree of freedom corresponding to rotation in the plane of the element. The element allows for large deformations but requires the strains to be small. The material properties were founded on tension tests of the steel sheets from which the profiles were fabricated. An isotropic, elastic-ideal plastic material model, von Mises yield criterion, with a yield stress of 385 MPa and Young's modulus of 212 GPa were adopted. Initial stresses in the profiles due to the forming procedure were not considered in the modeling.

3 Numerical simulations

The columns considered are employed as upright members in pallet racks. The length of the columns was set to 1250 mm which corresponds to a typical height of one compartment in a pallet rack in industry. In most cases, however, upright members are continuous without joints from the floor to the top of the rack. This, combined with the fact that the stiffness of the connectors at the floor and at the horizontal beams varies from one racking system to another, makes it difficult to achieve appropriate and generally applicable boundary conditions for the columns. Therefore only the extreme cases, rigid supports and pin-ended supports, were dealt with. In all the simulations performed, warping and distortion of the cross sections were prevented at the ends of the columns.

Each simulation was divided into a number of displacement-controlled preloading steps where the columns were damaged laterally by indentation of a rigid body, and an axial compression step where the remaining load-carrying capacity was evaluated. The simulations were divided into three groups with different boundary conditions and load cases. Simulations I and II consider impact normal to the broad side. In simulation I the columns are rigidly supported and in simulation II the columns are pin-end supported. Simulation III considers impact to the corners of the columns with pin-ended supports. Each simulation was performed for all three profiles, and different magnitudes of damage were considered.

3.1 Simulation I

The preloading, damaging part of this simulation was divided into three steps. Fig. 2 shows these steps and the consequent axial compression. First the broad side at the middle of each column was indented by a rigid body pressed normally to the broad side. The thickness of the rigid body was 40 mm but the

edges were rounded off with a radius of 5 mm so that only 30 mm initially came in contact with the structure. There was no friction between the rigid body and the deformable structure. The columns were supported so that they were free to rotate around the in-plane axis of the cross section, parallel to the broad side (dotted axis in the left part of Fig. 2) but no twisting was allowed around the normal of the cross section at the ends. Then the rigid body was released and lost contact with the structure. In the third step the ends of the columns were bent so that the cross section normals at the supports ended up parallel to the original upright axis. The reason why the ends were bent back to their original orientation in a separate step was that the alternative, to keep the ends rigid from the beginning, would yield a highly unstable behavior of the column when the rigid body was released in the second load step. Elastic energy would rapidly be released and thus cause major numerical difficulties. However, if a dynamic analysis had been carried out it would probably be possible to deal with that behavior as the mass inertia would contribute to stabilize the structural response.

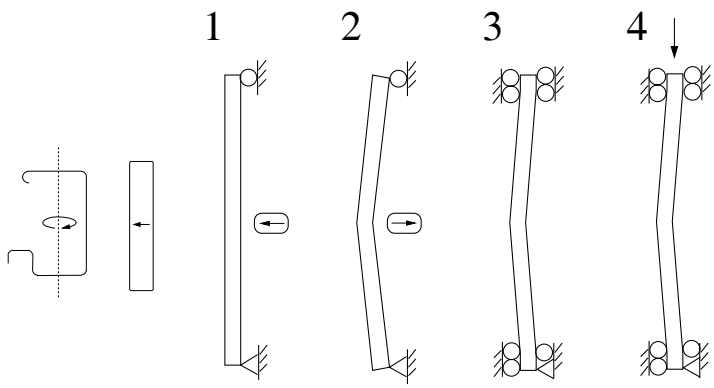

Fig. 2. *Boundary conditions and load steps in simulation I.*

The extent of the damage was represented by the average of the displacements of two nodes, in the middle of each column in the direction normal to the broad side. The nodes are indicated in Fig. 3 where the deformations of the midsections are also shown for 10 mm damage. Fig. 4 shows the entire columns with the same magnitude of damage. The preloading part of the simulation also initiated the mode of failure for the columns and, as shown in Figs. 3 and 4, all three profiles failed in a combination of flexural and distortional buckling.

In the final step, axial compression was applied to the columns. Different magnitudes of damage, caused by the preloading steps, resulted in different reductions of the load-carrying capacity. Fig. 5 shows the axial load-carrying capacity as a function of the damage magnitude for the three profiles. A value of 100% corresponds to the load-carrying capacity of undamaged columns,

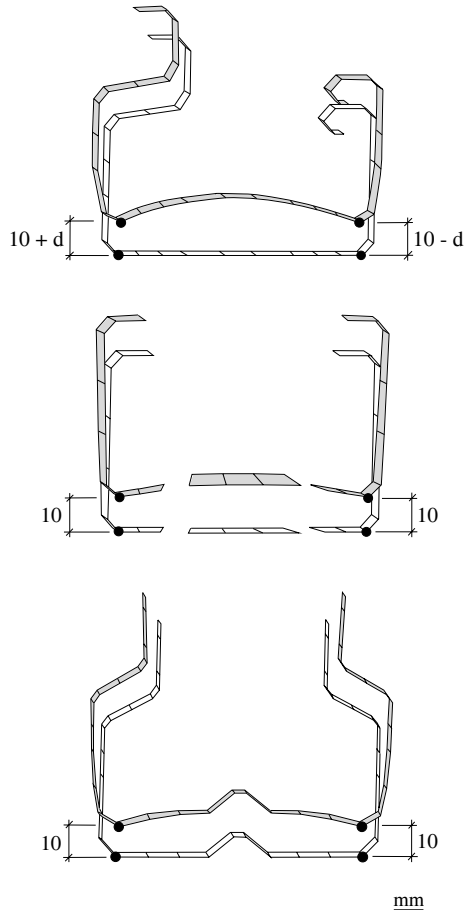

Fig. 3. *Deformed cross sections.*

which for the asymmetric profile was 183 kN, for the C profile 173 kN, and for the Ω profile 187 kN. The asymmetric profile and the Ω profile were affected by damage in the same extent. The load-carrying capacity was reduced by 50% for damage of approximately 12 mm.

The C profile did not lose as much load-carrying capacity as the other profiles for small damage, but when the rigid body displacement in the first preloading step was increased over a certain magnitude (40 mm) the cross section of the C profile distorted substantially during the third preloading step. This resulted in severe damage, but the representation of damage as defined was not able to capture the distortional part of the deformation. To capture this behavior, it would be necessary to introduce a more sophisticated definition of damage. However, it would then be cumbersome to compare the effects of damage to different profiles as the definition of damage would differ. It would also be more complicated to use the computational results to evaluate the influence

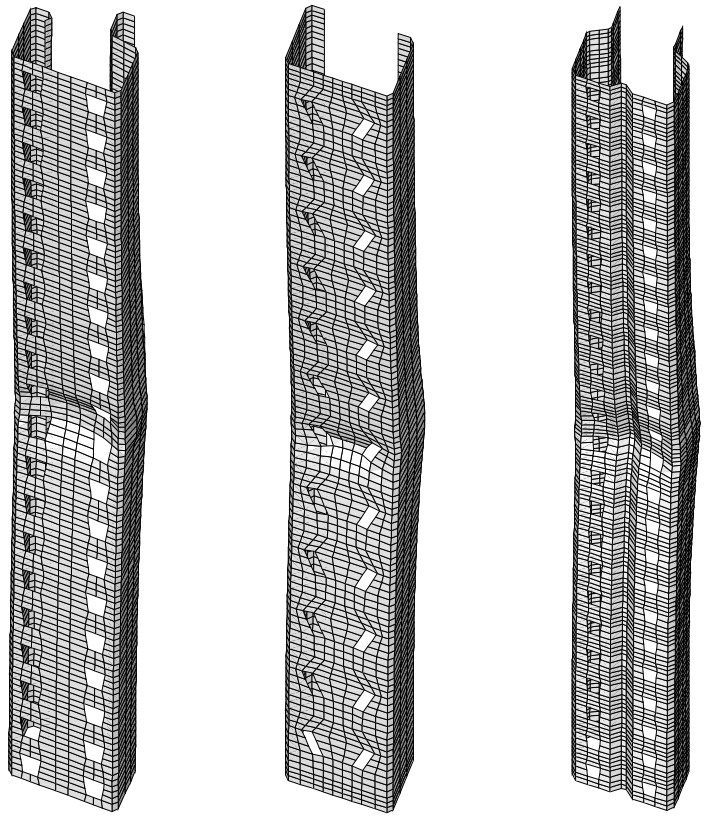

Fig. 4. *Columns with 10 mm damage.*

of damage to columns in industrial racking systems.

The axial compression stiffness was also affected by damage. Fig. 6 shows, for the asymmetric profile, the axial force as a function of the axial compressive deformation for a number of different damage magnitudes, 0–12 mm in steps of 2 mm. The stiffness decreased with increasing damage magnitudes. However, it can also be seen in Fig. 6 that the load-carrying capacity at the maximum loading was less sensitive to additional axial compressive deformation for columns with large damage. This is an advantageous quality in statically indeterminate systems which are able to redistribute the paths of the loading to other parts of the structure when some structural members are damaged.

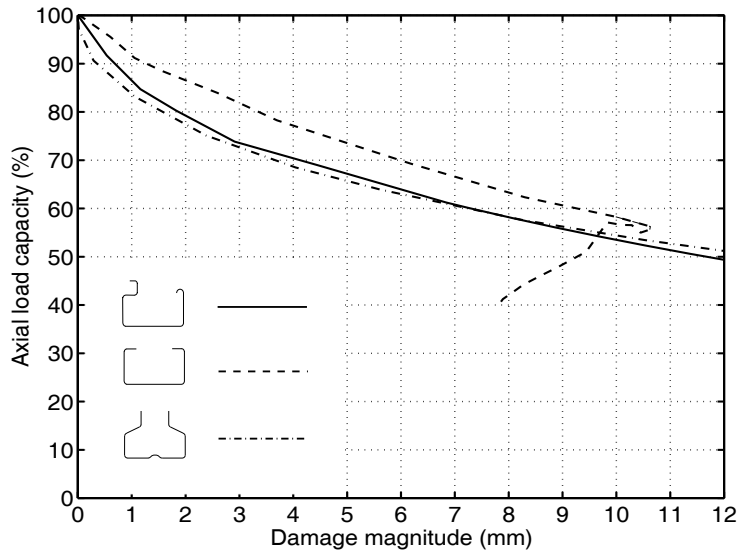

Fig. 5. *Load-carrying capacity as function of damage magnitude (simulation I).*

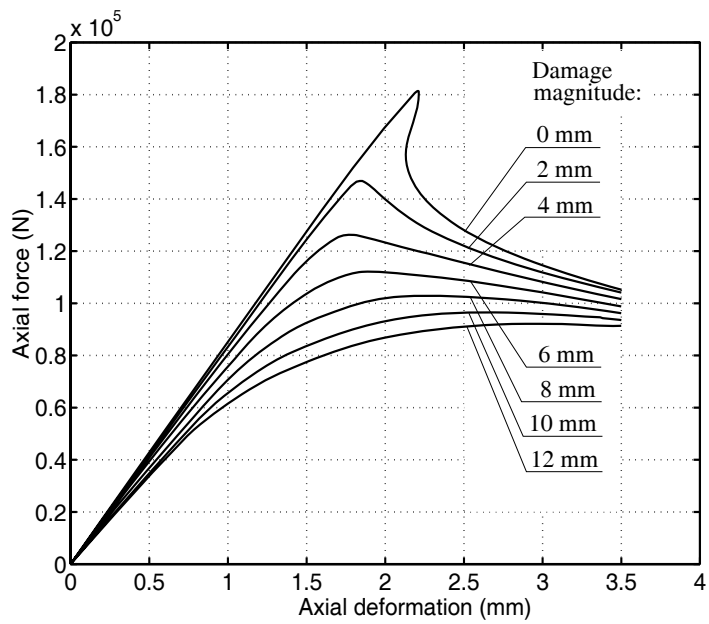

Fig. 6. *Axial force as function of axial compression for the asymmetric profile.*

3.2 Simulation II

The preloading part of this simulation was divided into two steps, identical with the first and second steps of the previous simulation. Thus the boundary conditions allowed the columns to rotate around the axis parallel to the broad side when the axial compression step was applied. The extent of damage was represented as before with the displacements of two nodes at the middle of each column, but the damage magnitude was determined after the second preloading step (Fig. 2). The magnitudes of the different modes of deformation increased almost in proportion to the damage, and it was possible to achieve much higher damage magnitudes than with the previous simulation. Fig. 7 shows the axial load-carrying capacity of the different profiles as a function of the damage magnitude. The 100% load-carrying capacity corresponds to 142 kN for the asymmetric profile, 131 kN for the C profile, and 169 kN for the Ω profile. The reduction of load-carrying capacity due to different damage magnitudes was roughly the same for all the profiles. As in the previous simulation, damage of 10–12 mm resulted in reduction of the load-carrying capacity of 40–50%. Damage of 20 mm resulted in approximately 60% reduction of the load-carrying capacity.

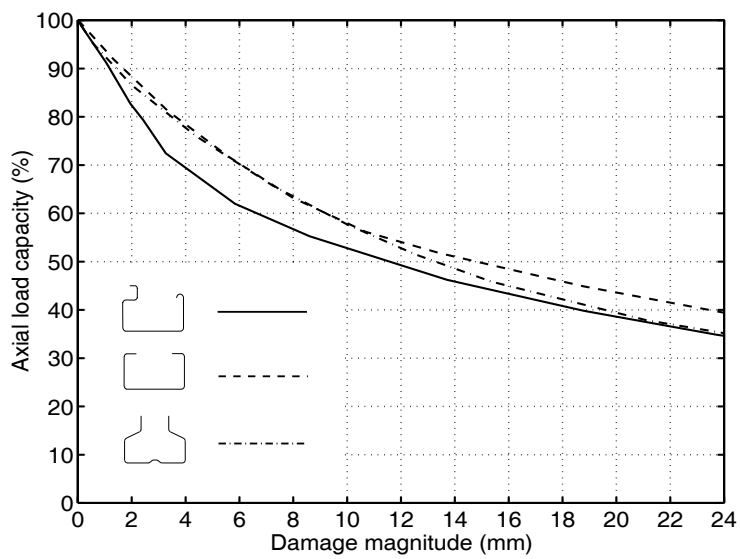

Fig. 7. *Load-carrying capacity as function of damage magnitude (simulation II).*

This simulation was performed to investigate the effects of damage caused by impacts to the corners of the profiles. Fig. 8 shows the steps in the simulation. In the first preloading step a rigid body was pressed laterally to the corner of each column at an angle of 45° to the broad side. The supports allowed the columns to rotate around the axes normal to the upright axis, but no twisting was allowed around the upright axis. Then, in the second step, the rigid body was released. Damage was defined as the displacement, in the plane of the cross section, of the indented corners when the second preloading step was completed. Damage of different extent consisted mainly of bending of the columns, and only moderate distortion of the cross sections occurred. Damage was therefore sufficiently represented by the adopted definition.

As in the previous simulations, the columns were compressed through the centroidal axis in the final load step. Fig. 9 shows the axial load-carrying capacity as a function of the damage magnitude. The 100% load-carrying capacity corresponds to 115 kN for the asymmetric profile, 131 kN for the C profile, and 169 kN for the Ω profile. As the axis parallel to the broad side coincide perfectly with the minor axes of inertia for the symmetric profiles, the load-carrying capacities of those columns were equal to those of simulation II. For the asymmetric profile, however, the load-carrying capacity was 19% lower due to the difference in boundary conditions.

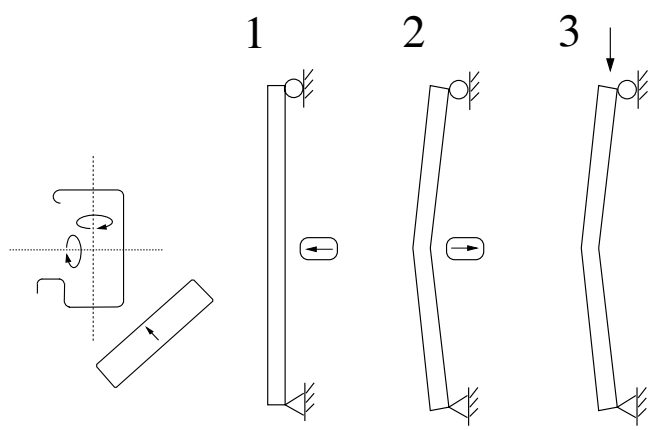

Fig. 8. *Boundary conditions and load steps in simulation III.*

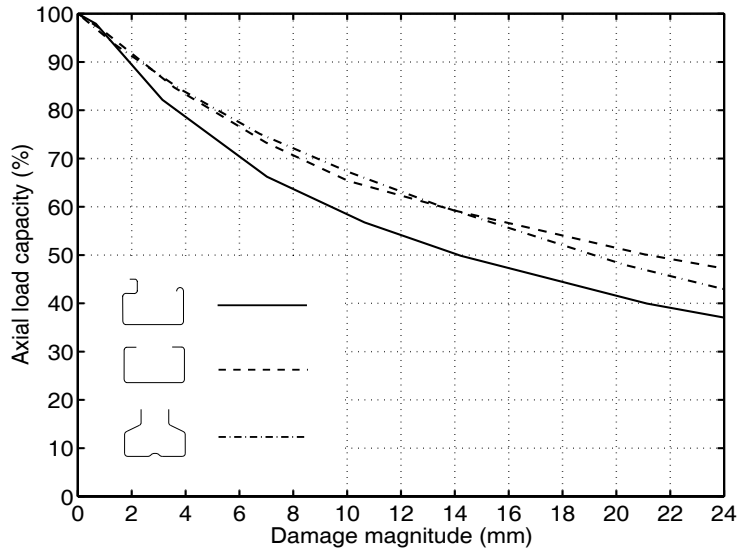

Fig. 9. *Load-carrying capacity as function of damage magnitude (simulation III).*

4 Experimental verification

To evaluate the reliability of the numerical simulations, a laboratory test series was performed. Only the profile with asymmetric cross section was tested, and only one set of boundary conditions was considered. Furthermore, the test series was restricted to six 1250 mm long specimens, of which four were exposed to damage before the axial load-carrying capacity was evaluated.

4.1 Test setup

The ends of each specimen were welded to rectangular steel plates with edges parallel to the broad side of the profile. The arrangement consisted of a preloading part and an axial compression part. In the first step of the preloading, a solid steel bar, with the same dimensions as the rigid body in the numerical simulations, was pressed to the broad side as indicated in Fig. 10. In the second step, the steel bar was released and the damage magnitude, as previously defined, was recorded. In the last step of the test, the specimen was put into axial compression as shown in Fig. 11. It was compressed through the centroidal axis, and a small ball, 28.5 mm in diameter, was placed between two steel plates at each support so that the ends of the profile were free to rotate in any direction.

Fig. 10. *Compression of a steel bar to the broad side of a column.*

Fig. 11. *Axial compression of a damaged column.*

The boundary conditions in the experimental arrangement differed slightly from those in the second numerical simulation. To imitate the conditions during the test series as closely as possible, an additional simulation was performed. The steps are shown in Fig. 12. In the first preloading step, a rigid body was pressed to the broad side of the profile. The ends of the columns were free to rotate around the axes normal to the upright axis. In the second step, the rigid body was released and the columns were free to rotate around the upright axis as well. Finally, the columns were compressed through the centroidal axis while the boundary conditions allowed them to rotate as in the second load step.

The material parameters were, as previously, evaluated from tension tests of small specimens of steel sheet. However, the properties of specimens from the same delivery as the columns used in the laboratory test series differed from those previously adopted. Due to these new material tests, the yield stress was 15% lower (328 MPa instead of 385 MPa) in this simulation than in simulations I–III.

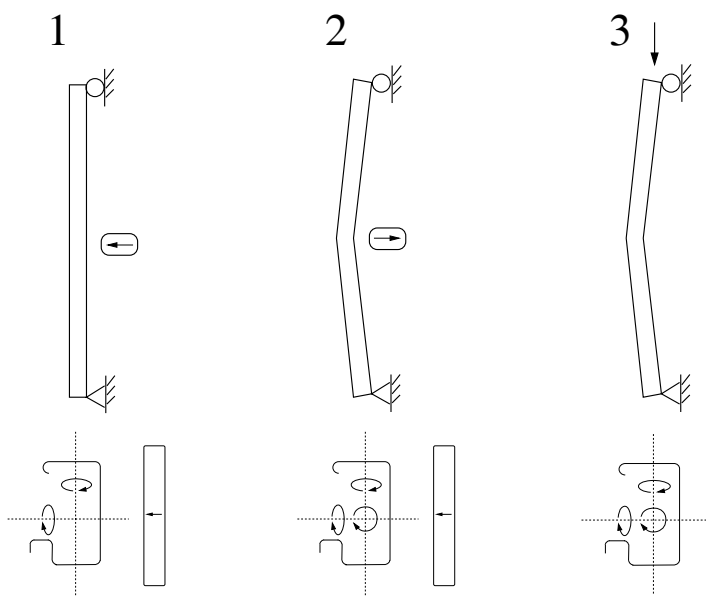

Fig. 12. *Boundary conditions and load steps in the comparative simulation.*

4.3 Results

The results of the laboratory test series in terms of the axial load-carrying capacity, and the corresponding damage magnitudes, are shown in Table 1. The reduction in load-carrying capacity in percent of the capacity of the undamaged column, according to the comparative computer simulation, is also shown. Specimens one and two were not exposed to any preloading, but even the undamaged columns were a little curved, giving displacements of the mid-sections in relation to the ends. This is equivalent to damage according to the definition. Specimens three and four were aimed to receive damage of 15 mm, and specimens five and six were aimed to receive damage of 20 mm. Guided by the numerical simulations, the displacement controlled lateral impress of the steel bar was 10 mm deeper than the desired damage magnitudes.

The results from the numerical simulation were in good agreement with the laboratory test series. Fig. 13 shows the results of the test series and the corresponding simulation. The test specimens are represented by the circles, and the computational results are represented by the curve. The load-carrying capacity is shown as a function of the damage magnitude. The 100% load-carrying capacity corresponds to 103 kN, which was the load-carrying capacity for an undamaged column according to the numerical simulation.

Specimen	Damage[a] (mm)	Capacity[b] (kN)	Reduction[c] (%)
1	0.4	97	−5.4
2	0.5	102	−0.5
3	13.6	63	−38.5
4	14.2	57	−44.4
5	21.8	45	−56.1
6	18.9	51	−50.2

Table 1. *Load-carrying capacity of columns with different damage magnitudes.* [a] *Damage magnitude.* [b] *Load-carrying capacity according to laboratory test.* [c] *Reduction in load-carrying capacity compared to undamaged column in comparative computer simulation.*

5 Conclusions

Thin-walled steel columns with channel sections damaged by truck impacts are treated in this paper. The study comprised a C profile, an Ω profile, and a profile with asymmetric cross section. Numerical simulations and a verifying laboratory test series were presented. The numerical simulations considered

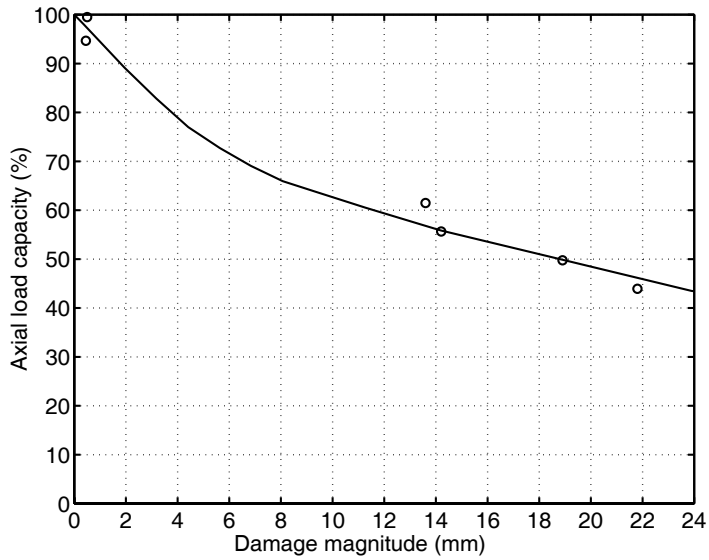

Fig. 13. *Load-carrying capacity according to the laboratory test series, and the corresponding numerical simulation.*

impacts in different directions, for rigid supports as well as for pin-ended supports.

The different profiles were affected by damage to approximately the same extent. For example, it was found that damage corresponding to 10 mm displacement of the midsections of columns with length of 1250 mm resulted in 33–47% reduction of the axial load-carrying capacity. The lower value corresponds to the Ω profile damaged by a rigid body pressed laterally to the column at an angle of 45° to the broad side of the cross section, simulation III. The higher value corresponds to the asymmetric profile damaged by a rigid body pressed laterally to the column in direction normal to the broad side of the cross section (simulation II). The mode of failure for the columns where for all three profiles a combination of flexural and distortional buckling.

The laboratory test series only comprised the asymmetric profile. Damage of 0–22 mm was tested and the results, both in terms of load-carrying capacity and deformation modes, were in good agreement with the results of the corresponding numerical simulation. The work presented in this paper is aimed at increasing the knowledge about how damage to upright members in pallet racks affects their load-carrying capacity, and to increase safety at the working sites where pallet racks are used. Effort is made to present the results in terms that are easy to relate to actual damage in industrial rack and shelving systems.

6 Acknowledgements

The work was financially supported by the Swedish Council for Work Life Research and carried out in cooperation with the Swedish National Testing and Research Institute. The authors gratefully acknowledge the contributions of Krystoffer Mroz, MSc., at the Swedish National Testing and Research Institute, and Karl-Gustav Carlsson, MSc., at Constructor Sweden AB concerning the contents and scope of the study.

Some earlier work concerning the load-carrying capacity of pallet racks is presented in Mroz (1995), and in Olsson and Sandberg (1998).

7 References

ABAQUS. (1996). Hibbitt, Karlsson, and Sorensen, Inc., Pawtucket, R.I.

Clarke, M. J. (1994). "Chapter 6: Plastic-zone analysis of frames." *Advanced analysis of steel frames: Theory, software, and application*, W. F. Chen and S. Toma, eds., CRC Press, London.

Davies, J. M., and Leach, P. (1992). "Some applications of generalized beam theory." *11th Int. Spec. Conf. on Cold-Formed Steel Struct.*, Center for Cold-Formed Steel Structures, University of Missouri-Rolla, St. Louis, 479–501.

Hancock, G. J. (1985). "Distortional buckling of steel storage rack columns." *J. Struct. Engrg.*, ASCE, 111(12), 2770–2783.

Mroz, K. (1995). "Load-carrying capacity of pallet racks." *SP Rep. 1995:07,* Build. Technol., SP-Swedish National Testing and Research Institute, Borås, Sweden.

Olsson, A., and Sandberg, G. (1998). "Parameter studies on pallet racks." *Rep. TVSM-7122,* Div. of Struct. Mech., Lund Institute of Technology, Lund, Sweden.

Rasmussen, K. J. R., and Rondal, J. (1997). "Strength curves for metal columns." *J. Struct. Engrg.*, ASCE, 123(6), 721–728.

Schardt, R. (1989). *Verallgemeinerte Technische Biegetheorie (Generalized beam theory).* Springer, Berlin (in German).

Paper 2

Failure Sensitivity Analysis of Engineering Structures

Göran Sandberg and Anders Olsson
Division of Structural Mechanics
Lund Institute of Technology

Failure Sensitivity Analysis of Engineering Structures

Göran Sandberg and Anders Olsson

Division of Structural Mechanics, Lund Institute of Technology, Lund University, P.O. Box 118, SE-221 00 Lund, Sweden

Abstract

The present paper suggests a method to consider uncertainties in engineering structures in a computational scheme. Latin hypercube sampling is used to prepare input data of probabilistic parameters for subsequent deterministic simulations where the mechanical response is evaluated. The approach is applied on a pallet rack system where damaged columns and connector stiffnesses are considered as probabilistic parameters. The mechanical simulations are performed with the finite element method, and full advantage is taken of existing commercial code.

Keywords: Finite element method, Sensitivity analysis, Uncertainties, Probabilistic parameters, Latin hypercube sampling, Pallet rack

1 Introduction

Computational mechanics has led to elaborate deterministic numerical methods and models, including sophisticated strategies for dealing with a variety of mechanical processes. Nowadays it is common practice in the design of engineering structures to rely on computational analysis. However, in most design cases the engineer is left with uncertainties about how to actually model a structure. The uncertainties can be directed towards the stiffness values of structural members or connections, or geometrical or material properties. Also production errors or damage, caused by accidents or inadequate management, are in many civil engineering structures uncertain parameters that should be considered in the analysis. Another question is how the load is applied and, in dynamic analysis, the time history of the load.

There is a growing realization that unavoidable uncertainties must be considered in a computational scheme to produce reliable computational and engineering results. Traditionally, designers have used safety factors to provide in-

creased confidence in the structural performance. However, this approach does not take into account the underlying, more sophisticated probability characteristics and does not provide the designer with adequate information about the reliability. This has lead to rather extensive research aiming to combine efficient methods of structural analysis with stochastic analysis where the influence of random variables is evaluated.

The finite element method, which is the dominating numerical tool in deterministic analysis, is the basis of many methods involving random parameters. Stochastic finite element approaches are based on the representation of stochastic fields as a series of random variables. The probabilistic design parameters are represented in the system matrices, often at the element level, by submatrices containing the nominal or mean values of the uncertain parameters and other submatrices considering the perturbation of the parameter values. The size of the system matrices increases rapidly with the number of probabilistic parameters and the order of the series expansion, see e.g. Jensen [1]. Kleiber and Hien [2] give a theoretical background in stochastic finite element analysis. The applicability of these methods is, however, limited since they in most cases are not capable of dealing with problems involving non-linearities or dynamic loading. Furthermore they are accurate only for small values of variability of the stochastic properties. Many methods also place restrictions on the element mesh.

A simple and widely used strategy for dealing with probabilistic parameters is Monte Carlo Simulations. The probabilistic input parameters are sampled from their distributions and a number of deterministic computations are performed to provide information about the distribution of the output parameters. This approach is the most accurate one and it is able to handle any mechanical processes which the deterministic methods are dealing with. The disadvantage is the computational cost, frequently very high due to the repeated analyses that have to be performed. In order to keep the computational cost low and be able to handle complex mechanical processes, combinations of stochastic finite element approaches and Monte Carlo simulations are suggested, see e.g. Papadrakakis and Papadopoulos [3]. A remaining disadvantage, however, common for most probabilistic methods, is the need for considerable revision in the finite element software developed for deterministic analysis.

In the present paper a Monte Carlo simulation approach, based on the Latin hypercube sampling plan, is applied to analyse the failure sensitivity of a complex civil engineering structure in an efficient manner. Latin hypercube sampling gives a good representation of the input distribution with proportionately few samples. The structure considered is a pallet rack system of a type frequently used in industry. The influence of damage to thin-walled steel columns and the influence of variations in connector stiffnesses are investigated. The sampling plan is only used to prepare the input data for the

subsequent analyses. Thus the influence of uncertainties are evaluated without any revision of the deterministic finite element code, in this case ABAQUS [4]. The present procedure is aimed not only towards advanced and unique problems, but also towards everyday engineering design practice.

Sensitivity has a precise mathematical significance. In this paper, however, sensitivity is more of system sensitivity for engineering structures. Thus it has here a more general meaning.

2 Latin hypercube sampling

The Latin hypercube sampling plan was theoretically described in 1979 in a paper by McKay et al. [5]. The desired accuracy in the estimated distribution function determines the required number of simulations. Let n denote the required number of simulations and k the number of uncertain parameters; the sampling space is then k-dimensional. The sampling plan is constructed as follows. For each of the k parameters, divide the outcome into n intervals with equal probability of occurrence and construct a column matrix with permutations of the integers $1, 2, \ldots, n$. Note that two such matrices can be identical. By putting the column matrices together, an $n \times k$-matrix is obtained. Each row in that matrix defines a k-dimensional hypercube cell in the sampling space. Take one random sample from each such cell. For two input variables with a uniform (0,1) distribution and five simulations, a possible sampling plan is shown in Fig. 1. Note that the samples are spread over the entire sampling space as the generation of the Latin hypercube sampling plan requires one sample from each row and each column. If n samples from the entire sampling space had been chosen completely at random, there is a risk that they would form a cluster and some parts of the sample space would not be investigated. For sampling in higher dimensions than three it is not possible to visualize the sampling plan, but it is clear that n samples spread over the whole sampling space are obtained. An interesting overview on different sampling plans is found in Kjell [6], and applications to structural analysis are suggested in Sandberg et al. [7].

3 Load-carrying capacity of pallet racks

The development of pallet racks and other load-carrying systems is undergoing a rapid growth, and progressively higher pallet racks are being designed. The development is requested by industry, and the competition between different manufacturers makes it necessary to minimize the cost of materials and production. Uncertainties in strength and stiffness of different structural members

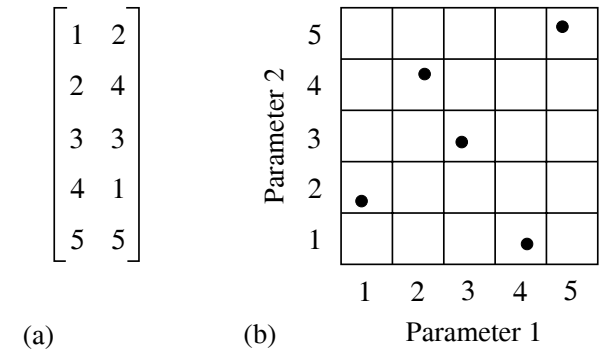

Fig. 1. *Latin cube, two parameters and five calculations. The* 5×2 *matrix (a) determines the plan illustrated in (b).*

occur and cause uncertainties in the structural performance. This results in difficulties in achieving valid guarantees of the load-carrying capacity. To preserve the safety and serviceability at the working site, additional knowledge concerning the mechanical behaviour and the influence of changing different parameters in pallet racks is therefore needed.

In this paper the influence of two different parameters are studied with respect to the load-carrying capacity. At first the effect of damage to thin-walled steel columns with open cross-sections is evaluated. Damage could for instance be caused by trucks running into the columns. The study comprises a close, deterministic investigation of the reduction in load-carrying capacity of individual columns due to different damage levels, and a global, probabilistic analysis of the influence of damaged columns in an entire pallet rack system. The analysis of the local, single column, level is only briefly discussed in this paper, see Olsson and Sandberg [8] for further details. The second parameter is the stiffness of the connectors between columns and horizontal beams. The influence of variations in stiffness between different connectors is investigated.

3.1 Damaged thin-walled steel columns

A model of an upright profile is built up of shell elements. The model describes the geometry of the profile in detail and is able to capture both in-plane and out-of-plane deformation of the cross-section. An elasto-plastic material model is used, and large deformation theory is applied. The length of the column is 1250 mm, which corresponds to the height of one compartment in the global pallet rack considered in the following study.

Simulations are performed to apply damage of different magnitudes to the profile and evaluate the influence of damage on the axial load-carrying capacity. The first part of the simulation, divided into three steps, applies the

damage to the structure. At first the broad side at the middle of the column is compressed by a rigid body in direction normal to the broad side. There is no friction between the rigid body and the deformable structure. The column is supported so that it is free to rotate around the in-plane axis of the cross-section, parallel to the broad side. Then the rigid body is released and loses contact with the structure. If the compression was big enough to cause yielding in the material, there will be remaining deformations in the structure. Finally the ends of the column are bent so that the cross-sections at the supports end up normal to the original upright axis. Fig. 2 shows the result of these steps in the simulation, a damaged column. Depending on the magnitude of the rigid body compression, different damage levels are obtained. Damage is represented by the imperfection, or the displacement of the cross-section at the middle of the column.

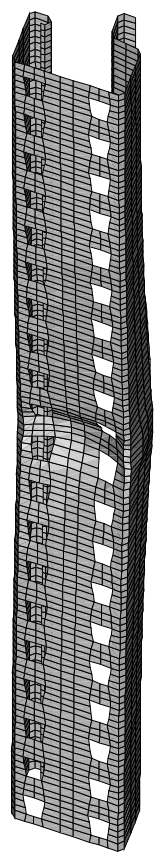

Fig. 2. *Damaged column according to the computer simulation.*

The second part of the simulation puts the column into axial compression. Fig. 3 shows the axial force as a function of the axial displacement for a number of columns with different damage levels (0–12 mm) and Fig. 4 shows the remaining load-carrying capacity as a function of the initial damage level. It is shown that even very small damage causes significant reduction in strength and stiffness. For example, a 12 mm imperfection causes a 50% reduction of the axial load-carrying capacity. However, to investigate the global influence of damage an entire pallet rack must be analysed.

3.2 Damaged columns modelled by beam elements

To achieve a reasonable size of the stiffness matrix of a global pallet rack model, the properties of damaged columns must be transformed from the shell model to a more simple beam model. In the shell structure, damage involved bending of the upright axis as well as in-plane deformation of the cross-section. To capture the effects of damage in the beam model, changes in two different characteristics are performed. The first change affects the geometry. An imperfection, equal to the damage level defined for the shell model, is introduced. This decreases the stiffness and strength of the beam structure, but not as mush as the corresponding damage in the shell structure. To adjust the damage effects, the material properties are involved. For increasing damage levels the yield stress of the material in the beam structure is decreased. The reduction of the yield stress is adjusted to achieve equal reduction in load-carrying capacity according to the different models. The calibration results in good agreement concerning axial stiffness, axial load-carrying capacity, and stiffness to bending. Fig. 5 shows the principal features of the calibration process.

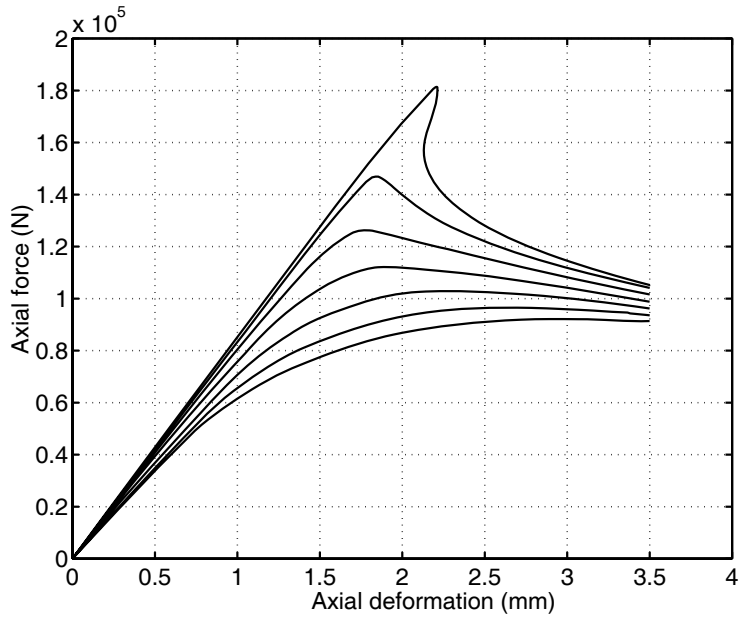

Fig. 3. *Axial force as a function of axial deformation.*

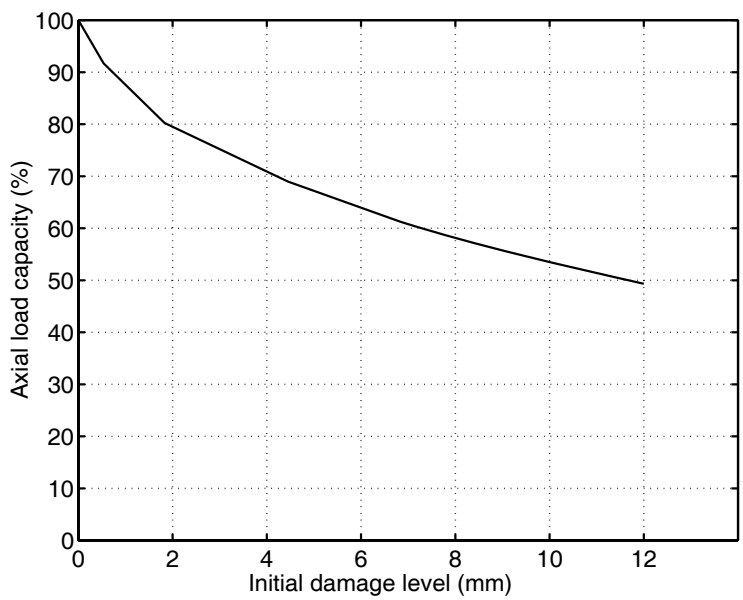

Fig. 4. *Remaining load-carrying capacity as a function of initial damage level.*

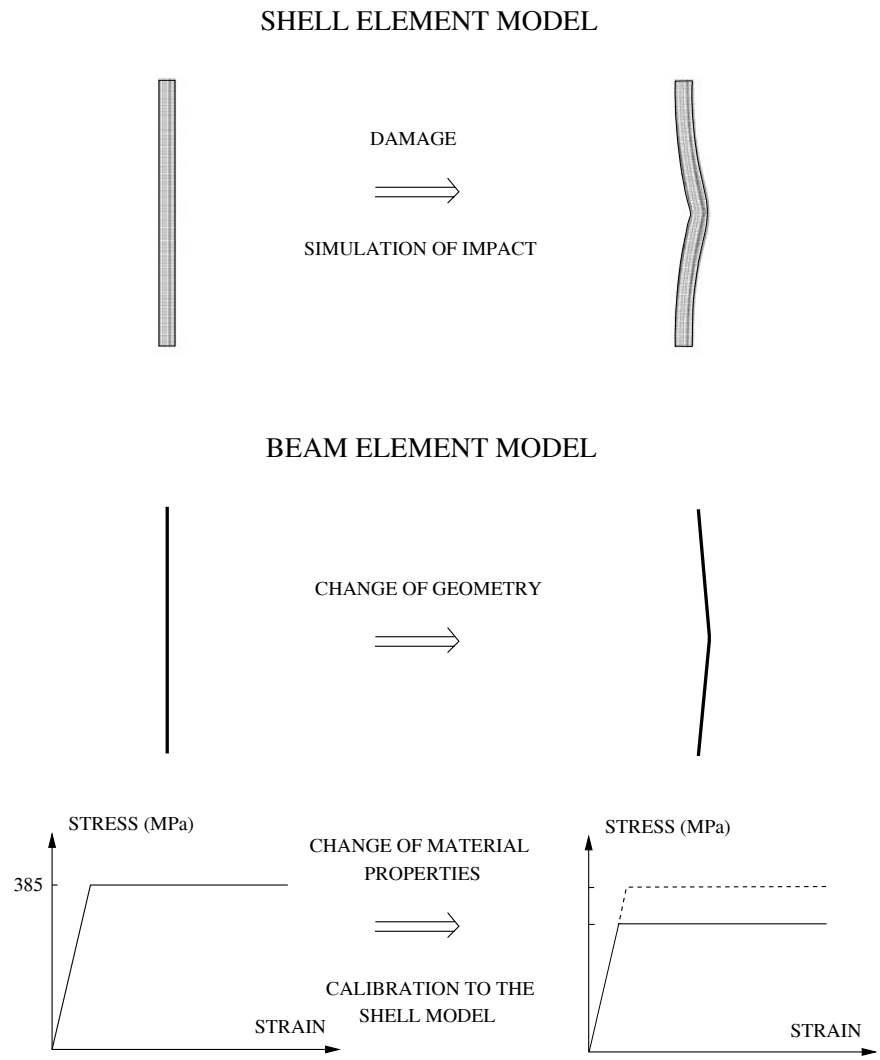

Fig. 5. *Damage as applied to the shell element model and to the beam element model.*

3.3 Global analysis of a pallet rack

The pallet rack in the present study contains five sections and four horizontal beam levels. Fig. 6 shows the geometry of the structure. The components in the pallet rack are typical for many racking systems used in industry. Laboratory tests, as well as numerical simulations, are performed to evaluate their mechanical properties, see Mroz [9].

The columns are modelled by beam elements which are able to capture torsion and warping of the cross-section. The horizontal beams are modelled by ordinary beam elements according to Timoshenko beam theory, and the diagonal elements, used for stabilization of the pallet rack in the cross-aisle direction, are modelled by truss elements, i.e. with pinned connections to the columns. The connections between the horizontal beams and the columns are modelled as finite elements with specified non-linear stiffness, evaluated from tests. The floor end connectors are modelled in the same manner. Large displacements are considered in the model as well as material non-linearities.

Fig. 7 shows the load configuration in the pallet rack. In the first load step the box loads and the corresponding horizontal loads are applied. Each box in the model represents a load of 10 kN and the horizontal loading amounts, in accordance with the FEM norm [10], to 0.31% of the vertical loading at the corresponding beam level. The pallet rack is also loaded by the weight of its own components. In the second load step the vertical loads at the columns at the top of the pallet rack and the corresponding horizontal loading are applied. The magnitude of the top loads is increased until failure occurs. Fig. 8 shows the three-dimensional structure of the pallet rack without damage, and the failure mode due to the loading applied, a global down-aisle sway mode.

3.4 Damage distribution in pallet racks

As the exact damage locations and damage magnitudes in a pallet rack are not known, it is not possible to perform an accurate deterministic computation to evaluate the influence of the damage. However, if the distribution of damage is known or can be estimated, this would be enough to perform a probabilistic analysis and find the distribution of the global load-carrying capacity. Inspections of pallet racks have shown that the main part of the damage is located in the lower parts of the pallet racks since impacts often occur there. It is also clear that the loading is bigger in the lower parts of the structure and damage there is likely to be of greater importance than damage in the upper parts of the structure.

In the present analysis it is assumed that every column in the lowest level

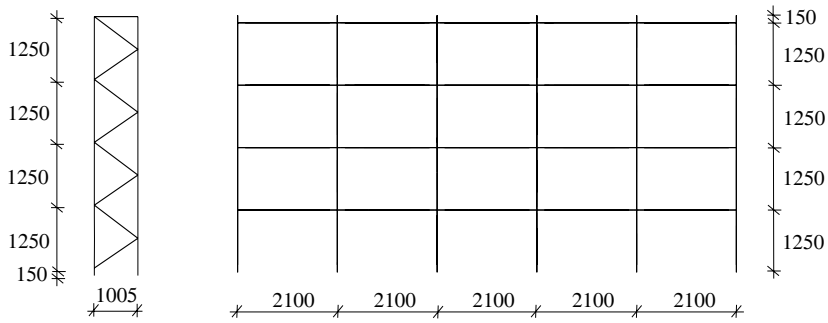

Fig. 6. *Geometry of the pallet rack. Lengths given in mm.*

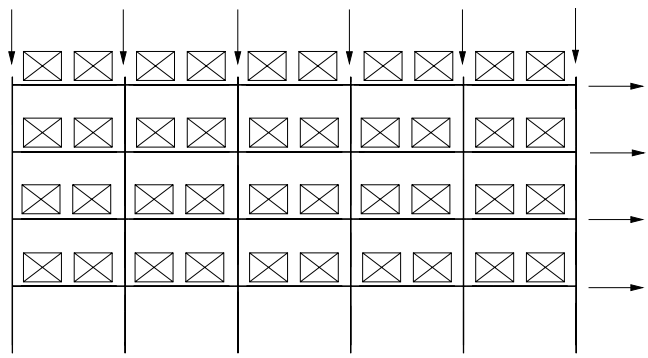

Fig. 7. *Load configuration in the pallet rack.*

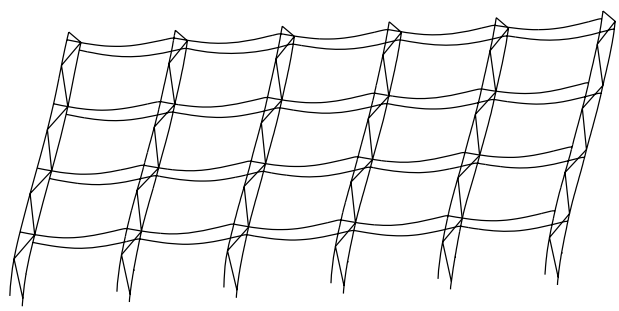

Fig. 8. *Failure mode for the pallet rack.*

of the pallet rack is damaged. The damage is of the type presented above and is located with equal distance to the floor and the lowest horizontal beam level. The damage magnitudes for the 12 columns are assumed to be uniformly distributed in the interval 0–12 mm.

3.5 Probabilistic analysis of global influence of damage

The Latin hypercube sampling plan is used to choose damage magnitudes for the 12 columns for a number of finite element simulations. The technique is already generally described, but the procedure for the present application is also presented with an example where input data to four deterministic computations are to be performed. Twelve columns are damaged, i.e. $k = 12$, and four different damage cases are considered, i.e. $n = 4$. The sampling space for the 12 parameters is divided into four intervals.

$$Intervals: \begin{bmatrix} 1 \\ 2 \\ 3 \\ 4 \end{bmatrix} \quad correlates\ to \quad \begin{bmatrix} 0 - \frac{1}{4} \\ \vdots \\ \frac{3}{4} - 1 \end{bmatrix}$$

Twelve permutations of the damage intervals are performed.

$$Perm.\ 1 = \begin{bmatrix} 3 \\ 1 \\ 4 \\ 2 \end{bmatrix} \quad Perm.\ 2 = \begin{bmatrix} 1 \\ 4 \\ 2 \\ 3 \end{bmatrix} \quad \cdots \quad Perm.\ 12 = \begin{bmatrix} 4 \\ 2 \\ 1 \\ 3 \end{bmatrix}$$

A matrix, four rows and 12 columns is established from the permutations.

$$\begin{bmatrix} 3 & 1 & \dots & 4 \\ 1 & 4 & \dots & 2 \\ 4 & 2 & \dots & 1 \\ 2 & 3 & \dots & 3 \end{bmatrix}$$

For each component, i.e. interval in the matrix above a random value is picked and multiplied by 12 mm. A new matrix is then established in which each line contains the damage magnitudes for the 12 columns for one deterministic computation.

$$\begin{bmatrix} 7.2 & 1.7 & \cdots & 9.2 \\ 1.9 & 11.6 & \cdots & 5.4 \\ 10.7 & 4.9 & \cdots & 0.8 \\ 3.4 & 7.1 & \cdots & 8.7 \end{bmatrix} \text{(mm)}$$

The damage magnitudes affect, as described above, the geometry and material for each of the 12 columns.

Fig. 9 shows the computational results in terms of the distribution of the load-carrying capacity for simulations with $n = 30$, $n = 100$ and $n = 300$. The load-carrying capacity is approximately uniformly distributed according to the simulations. The distributions become smoother when the number of samples increases, but even the 30-sample simulation gives a good representation of the variation of the load-carrying capacity. Failure arises for load levels between 0.68 and 0.86 (MN), where the latter value is equal to the failure load for a pallet rack without damage. The damage distribution causes a reduction in the load-carrying capacity of up to 20%. For all the damage cases considered in the simulations, the pallet rack fails in a global down-aisle sway mode as for a pallet rack without damage.

3.6 Stiffness of beam end connectors

Many pallet rack systems are designed without stabilizing bracing members in the down-aisle direction. The stiffness in that direction is then obtained with the framework of the horizontal beams and the columns. In this type of structures the stiffnesses of the beam end connectors are of vital importance for the behaviour of the pallet rack, and if failure occurs in a global down-aisle sway mode, as is the case for the pallet rack considered in this paper, the load-carrying capacity of the entire pallet rack is dependent on the stiffnesses of these connectors.

3.7 Connector stiffnesses as probabilistic parameters

There are always individual differences in the stiffness relations of the beam-end connectors in a structure. Usually mean values of stiffness and failure moment, including safety factors, are evaluated from tests of a number of specimens and used as design values for all the connectors in the structure. In this study the sensitivity with respect to the failure load is investigated when individual connector stiffnesses, picked from known distributions, are applied to the pallet rack model. Fig. 10 shows the bending moment as a function of

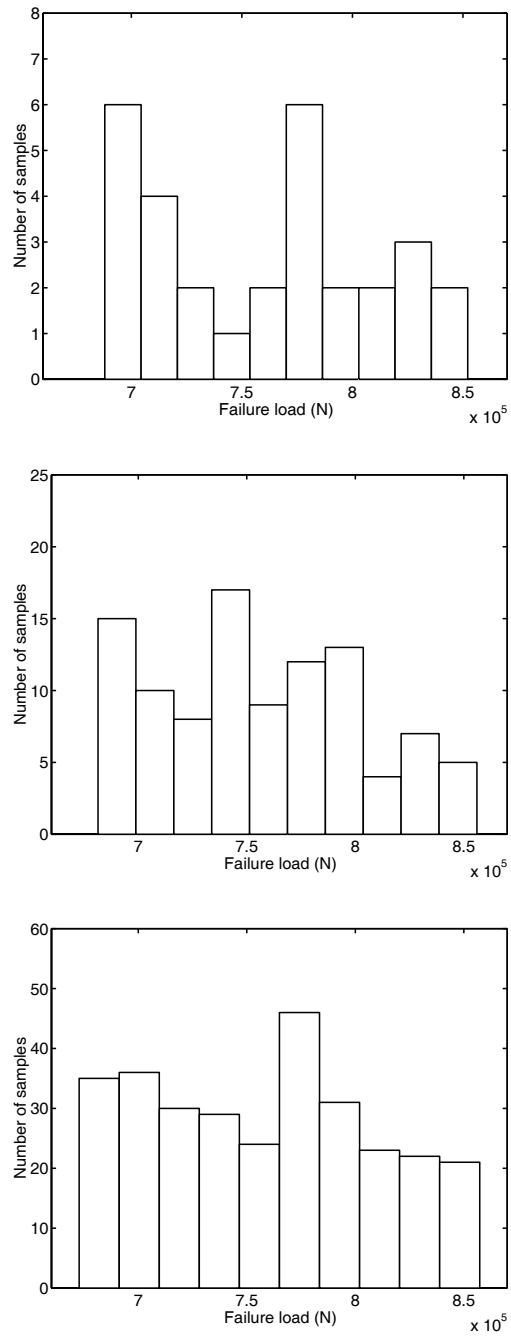

Fig. 9. *Distribution of the load-carrying capacity, with 30 samples, 100 samples, and 300 samples.*

the rotation for five specimens tested according to the recommendations in FEM [10]. Five specimens are too few to draw any reliable conclusions about the distribution of the stiffness, but the aim of this analysis is to illustrate a method to evaluate the distribution of the load-carrying capacity when the distribution of the connector stiffnesses is known. It is assumed that the bending moment, at a number of different rotations, is normally distributed. Mean values and standard deviations are then computed. Fig. 11 shows a schematic sketch of the mean stiffness curve evaluated from the curves in Fig. 10. The lengths of the vertical bars indicate the size of the standard deviations at different rotations. Each bar is divided into a number of intervals where all the intervals represent equal probability.

Latin hypercube sampling is used to produce an optional number of stiffness intervals. From the sampling plan each connector stiffness is only represented by one interval from the uniform (0,1) distribution, as in the preceding study on damaged columns, but in the finite element model each stiffness curve is defined by five rotations and five corresponding bending moments. To prepare each curve, five random values are picked from its interval and mapped on five normal distributions, with mean values and standard deviations evaluated from the laboratory test. The mapping is performed according to Eq. (1) and illustrated in Fig. 12.

$$N(r) = \sqrt{2}\sigma \; erf^{-1}(2r-1) + m \tag{1}$$

where

$$erf(2r-1) = \frac{2}{\sqrt{\pi}} \int_0^{2r-1} e^{-t^2} dt \tag{2}$$

In Eq. (1) σ is the standard deviation, m is the mean value, r is a random value from the current interval, and $N(r)$ is the value of r mapped on the normal distribution. If the sampling space is divided into four intervals, 4×80 stiffness curves are established. A possible result of the procedure for one connector is shown in Fig. 13.

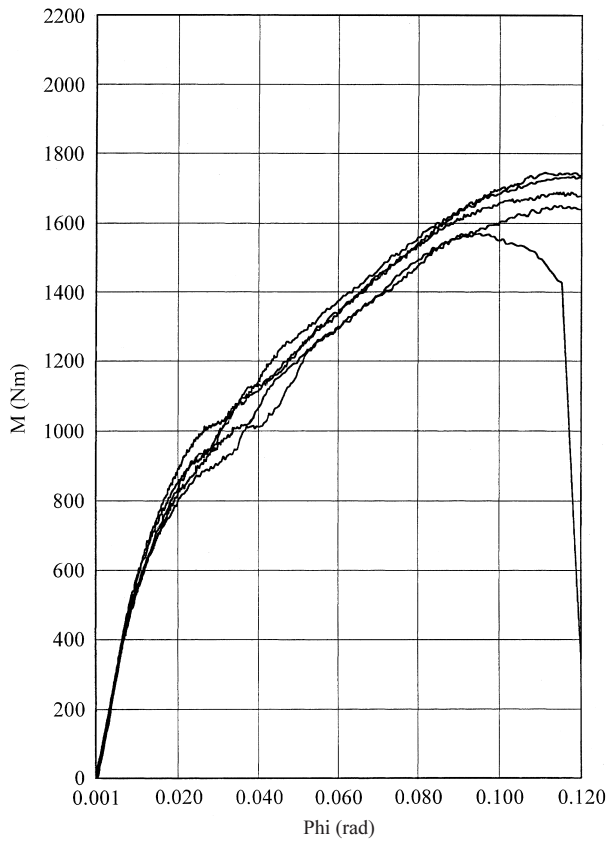

Fig. 10. *Stiffness curves of beam-end connectors according to laboratory test.*

3.8 Influence of variations in connector stiffnesses

Simulations with $n = 30$, $n = 100$ and $n = 300$ are performed. Fig. 14 shows the distribution of the load-carrying capacity according to the simulations, and Table 1 shows the mean values and the standard deviations of the connector stiffnesses and the load-carrying capacity. The standard deviation of the load-carrying capacity is very small compared to the standard deviations of the connector stiffnesses. This means that the global stiffness, and global load-carrying capacity are not very sensitive to variations around the mean values of the connector stiffnesses. This does not imply that the behaviour of the pallet rack is insensitive to variations of the mean value of the connector stiffnesses, but it could be concluded that in this particular case it is sufficient to treat the connector stiffnesses as deterministic parameters.

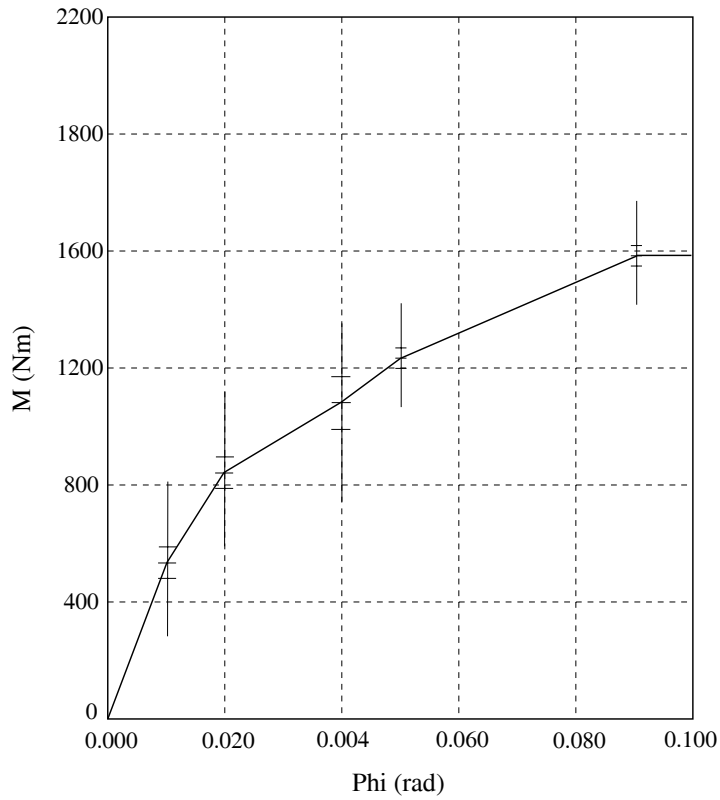

Fig. 11. *Mean stiffness curve of the beam-end connectors.*

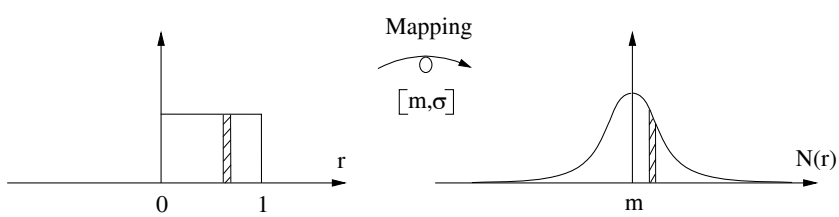

Fig. 12. *Mapping of a uniform distribution on a normal distribution.*

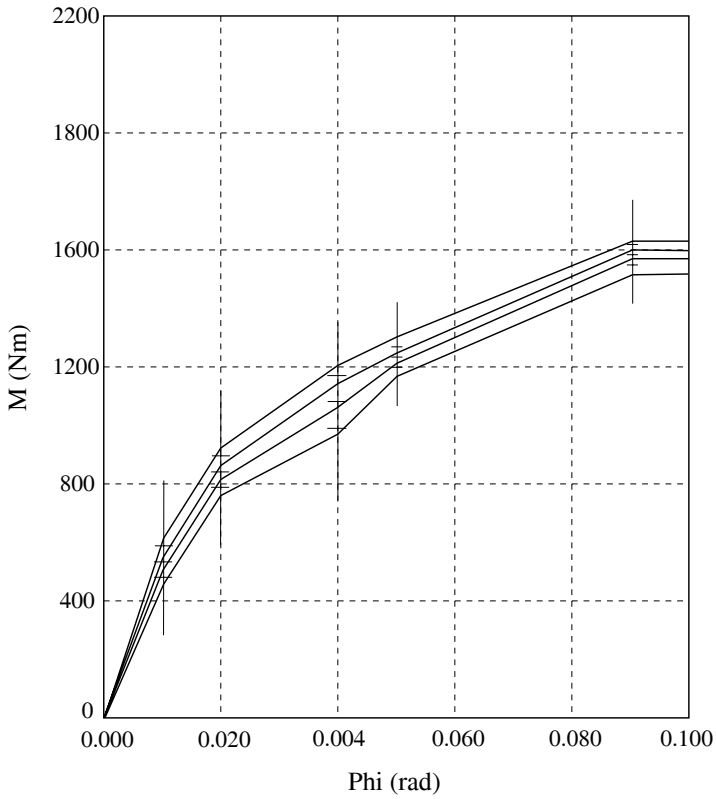

Fig. 13. *Possible generated stiffness curves.*

Parameter	Mean value	Standard deviation	
$M(\phi = 0.010$ rad)	559 Nm	18.6 Nm	3.3%
$M(\phi = 0.020$ rad)	838 Nm	31.0 Nm	3.3%
$M(\phi = 0.040$ rad)	1092 Nm	48.5 Nm	4.4%
$M(\phi = 0.050$ rad)	1222 Nm	35.7 Nm	2.2%
$M(\phi = 0.090$ rad)	1592 Nm	34.0 Nm	2.1%
L-c. c. 30 samples	865.9 kN	3.19 kN	0.37%
L-c. c. 100 samples	865.8 kN	2.38 kN	0.27%
L-c. c. 300 samples	865.6 kN	2.68 kN	0.31%

Table 1. *Mean values and standard deviations of connector stiffnesses and load-carrying capacity (L.c.c).*

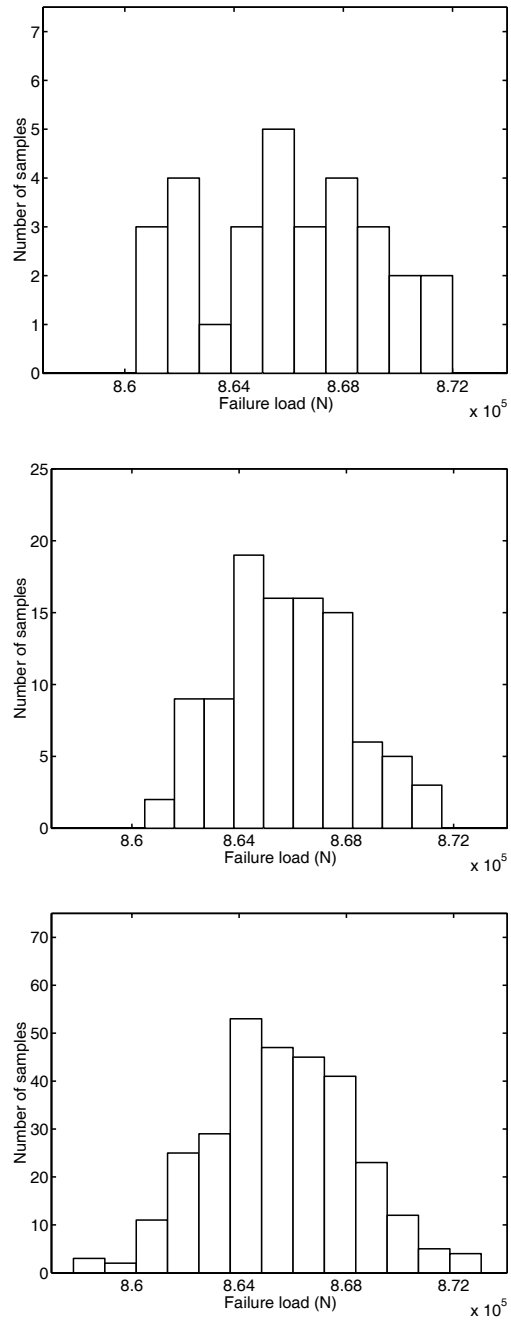

Fig. 14. *Distribution of the load-carrying capacity, with 30 samples, 100 samples, and 300 samples.*

4 Summary and conclusions

In this paper Latin hypercube sampling is used to prepare input data of probabilistic parameters to deterministic finite element analyses where non-linearities in structural behaviour are considered. An analysis of a pallet rack system shows that small damage to thin-walled steel columns is of great importance for the load-carrying capacity of the entire pallet rack as well as for the load-carrying capacity of individual columns. In a global pallet rack model damage is treated as a probabilistic parameter since it is impossible to predict the exact locations and magnitudes of damage. The simulation shows that damage corresponding to less than 12 mm imperfections causes reduction of the global load-carrying capacity of up to 20%.

The influence of deviations in the connector stiffnesses is also investigated. Laboratory tests of a few connectors are used to evaluate mean values and standard deviations of the stiffness relation. Synthetic stiffness curves are then generated and applied in the finite element model. The simulation shows that the global stiffness and thereby the load-carrying capacity are not very sensitive to deviations around the mean stiffness of the connectors.

The approach with Latin hypercube sampling allows the designer to analyse engineering structures, with probabilistic parameters, without keeping back the possibilities of using elaborate models and existing, deterministic codes. Compared to Monte Carlo simulations, where the samples are chosen completely at random, the representation of the distributions of the inputs are more accurate with the same number of samples.

References

[1] Jensen HA. A global sensitivity analysis in structural mechanics. Comput Struct 1995;56:903–15.

[2] Kleiber M, Hien TD. The stochastic finite element method. Chichester: Wiley, 1995.

[3] Papadrakakis M, Papadopoulos V. Robust and efficient methods for stochastic finite element analysis using Monte Carlo simulation. Comput Meth Appl Mech Engng 1996;134:325–40.

[4] Hibbitt, Karlsson, Sorensen. Inc. ABAQUS, Version 5.6., Pawtucket 1996.

[5] McKay MD, Conover WJ, Beckman RJ. A comparison of three methods for selecting values of input variables in the analysis of output from a computer code. Technometrics 1979;21:239–45.

[6] Kjell G. Computer experiments with application to earthquake engineering. Department of Mathematical Statistics, CTH, Studies in statistical quality control and reliability 1995 7, Gothenburg.

[7] Sandberg G, Kjell G, de Maré J. Computational planning using Latin hypercube sampling. Report TVSM-7118, Lund Institute of Technology, Division of Structural Mechanics, Lund 1997.

[8] Olsson A, Sandberg G. Parameter studies on pallet racks. Report TVSM-7122, Lund Institute of Technology, Division of Structural Mechanics, Lund 1998.

[9] Mroz K. Load-carrying capacity of pallet racks. SP report 1995:07, SP-Swedish National Testing and Research Institute, Building Technology, Borås 1995.

[10] Federation Européenne de la Manutention (pre Norm) Recommendations for the Design of Steel Static Pallet Racking (January 1996), Section X, Manchester 1996.

Paper 3

On Latin Hypercube Sampling for Stochastic Finite Element Analysis

Anders Olsson and Göran Sandberg
Division of Structural Mechanics
Lund Institute of Technology

On Latin Hypercube Sampling for Stochastic Finite Element Analysis

Anders Olsson and Göran Sandberg

Division of Structural Mechanics, Lund Institute of Technology, Lund University, P.O. Box 118, SE-221 00 Lund, Sweden

Abstract

The present paper suggests a Latin hypercube sampling method, with correlation control, for stochastic finite element analysis. This sampling procedure significantly improves the representation of stochastic design parameters compared to standard Monte Carlo sampling. As the correlation control requires the number of realizations to be larger than the number of stochastic variables in the problem, principal component analysis is employed to reduce the number of stochastic variables. In many cases this considerably relaxes the restriction on the number of realizations. Furthermore, it is an advantage to combine the sampling method with the well-known Neumann series expansion method for solving the equation systems efficiently. The paper comprises an extensive comparison of different sampling methods and perturbation methods for stochastic finite element analysis. It is shown that the Latin hypercube sampling plan, with correlation control, in conjunction with the Neumann series expansion method, is a competitive approach regarding computational efficiency as well as general applicability.

Keywords: Latin hypercube sampling, Finite element method, Correlation control, Principal component analysis, Neumann series expansion

1 Introduction

Nowadays elaborate deterministic numerical methods and models, including sophisticated strategies for dealing with a variety of mechanical processes, have become widespread and are employed in everyday engineering design practice. However, in most design cases the engineer is left with uncertainties about how to actually model a structure. The uncertainties can be directed towards geometrical or material properties and affect the strength and stiffness of structural members and connections. Production errors or damage, caused by accidents or inadequate management, are in many civil engineering

structures uncertain parameters that should be considered in the analysis as well. Other issues are how the load is applied and, in dynamic analysis, the time history of the load.

There is a growing realization that unavoidable uncertainties must be considered in a computational scheme to produce reliable computational and engineering results. Traditionally, designers have used safety factors to provide increased confidence in the structural performance, but this approach does not take into account the underlying, more sophisticated probability characteristics and does not provide the designer with adequate information about the reliability of the entire system. This has lead to rather extensive research aiming at combining efficient methods of structural analysis with stochastic analysis, where the influence of random variables is evaluated.

The only method that has become widespread in engineering design practice is the Monte Carlo simulation technique. Probabilistic design parameters are sampled and a number of deterministic computations are performed to provide information about the distribution, or some statistics of response parameters. This is an accurate and simple approach, but also very expensive in terms of computer resources. Several methods that could be employed at a lower computational cost have been proposed. These can be divided into three main categories. The methods of the first category concern the sampling itself of the Monte Carlo technique in order to reduce the number of realizations required to provide reliable statistics of the response. Stratified sampling and Latin hypercube sampling belong to this category. Most work in this area has been carried out by mathematical statisticians [e.g., McKay et al. (1979); Iman and Conover (1982); Stein (1987); Owen (1994); Harris et al. (1995); Kjell (1995)], and elaborate sampling techniques are rarely employed in the field of structural analysis using finite elements. A major advantage of these methods is that the consequent analyses, i.e. the runs determined by the sample, are identical to the deterministic analysis. Thus, full advantage can be taken of existing commercial code developed for deterministic analysis (Sandberg et al. 1997; Sandberg and Olsson 1999).

The methods of the second category also employ Monte Carlo simulations. However, the strategy is to reduce the computational work by using efficient solution techniques for the equation system of each run by making use of the similarity between the different realizations. The Neumann series expansion method, and the preconditioned conjugate gradient method belong to this category. The Neumann series expansion method in conjunction with the standard Monte Carlo method has been employed by several researchers and found to be efficient [e.g., Yamazaki et al. (1988); Chakraborty and Dey (1996)]. The preconditioned conjugate gradient method has been used in conjunction with the Neumann series expansion method, and the standard Monte Carlo method by Papadrakakis and Papadopoulos (1996).

Methods of the third category do not compute the response statistics through Monte Carlo simulations but through series expansions of random variables. The most well-known methods are probably: the Taylor series expansion method, in which a truncated Taylor series of the response variable is established (Liu et al. 1986; Kleiber and Hien 1992), the Neumann series expansion method, in which a truncated Neumann series is employed for the equation system (Shinozuka and Deodatis 1988; Spanos and Ghanem 1989), and the basis random variable method, in which the statistics of the response variables are evaluated by minimizing the potential energy of the system with respect to statistics of the basis random variables (Lawrence 1987). A comprehensive exposition of a wide range of stochastic finite element methods, from the second and third category, is given in Matthies et al. (1997).

The present paper makes a contribution to the first category of methods. The Latin hypercube sampling method, with correlation control, is further developed to overcome the restriction that the number of realizations must exceed the number of correlated random variables. The method can unimpededly be combined with methods from the second category. Furthermore, for the sake of completeness and in order to make some comments, the paper briefly describes the Neumann series expansion method in conjunction with Monte Carlo simulations, and the Taylor series expansion method in correlated as well as uncorrelated random variable space. Finally, by means of numerical examples, the suggested approach is compared to the alternative methods with respect to accuracy, efficiency, and general applicability.

2 Representation of random fields

This section contains some basics of the theory of random fields, and a brief account of the most commonly employed discretization methods in connection with finite elements. A thorough treatment of the theory of random fields is found in Vanmarcke (1984).

The random field, $H(\mathbf{x})$, of some physical property such as the Young's modulus, or the thickness of a plate can be expressed as the sum of its mean value function, $\mu(\mathbf{x})$, and its fluctuating component, $a(\mathbf{x})$, where $\mathbf{x}$ indicates the position vector,

$$H(\mathbf{x}) = \mu(\mathbf{x}) + a(\mathbf{x}) \tag{1}$$

The mean value is then a deterministic function of the spatial variables, whereby the fluctuating component is a random function, with a mean of

zero, of the same variables,

$$E[a(\mathbf{x})] = 0 \tag{2}$$

Furthermore, the random field is represented by the auto-covariance function,

$$C_{aa}(\mathbf{x}, \mathbf{x}') = E[a(\mathbf{x})a(\mathbf{x}')] \tag{3}$$

where $\mathbf{x}$ and $\mathbf{x}'$ are two locations in the variable space. Higher order expectations might also be employed in the modeling of the random field. However, it is convenient, and often sufficient, to confine the statistics to the mean value function and the auto-covariance function. For Gaussian fields these statistics unambiguously determine the distribution. If the random variation is assumed to be homogeneous, i.e. the covariance between two points depends only on the relative position, $\xi = \mathbf{x} - \mathbf{x}'$, the auto-covariance function can be expressed as

$$C_{aa}(\xi, \sigma_0) = \sigma_0^2 \ \rho_{aa}(\xi) \tag{4}$$

in which σ_0 is the standard deviation, the same at every location, and $\rho_{aa}(\xi)$ is an auto-correlation function with $\rho_{aa}(0) = 1$. Furthermore, if the random field is isotropic, i.e. the covariance between two points depends only on the distance, the auto-covariance function can be expressed as

$$C_{aa}(\xi, \sigma_0) = \sigma_0^2 \ \rho_{aa}(|\xi|) \tag{5}$$

It should be noted, however, that the finite element approaches presented herein are not limited to isotropic or homogeneous random fields.

The next step is to discretize the random field and its statistics to fit the consequent finite element analysis. Several discretization methods have been proposed. One of the most simple and widely employed is *the midpoint method* in which the value at the center point of each element is used to represent the random field within the element. Another point discretization method is *the integration point method* in which the integration points are used to represent the random field. These two methods have the advantages of yielding positive definite covariance matrices and to allow other marginal distributions than the Gaussian. The major disadvantage is that the finite element mesh has to be very fine in order to capture the correlation of the random field sufficiently, especially if the correlation length is short. Alternative methods are *the interpolation method*, which is based on representing the random field in terms of an interpolation rule involving a set of deterministic shape functions and the random nodal values of the field, and *the local averaging method*, which

integrates the random field function over each element or domain. These latter methods are able to represent the random field with coarser meshes than the point discretization methods, but they are strictly valid only in the case of Gaussian random fields. Also, the local averaging method might in some cases lead to non-positive definite covariance matrices. More detailed descriptions, and several references on random field discretizations are given in Matthies et al. (1997).

The discretized random field is now represented by the mean value vector, and the covariance matrix, corresponding to the mean value function, and the auto-covariance function of the undiscretized random field. Using the mid-point method, the length of the mean value vector and the number of rows and columns in the symmetric covariance matrix are equal to the number of elements in the problem. The mean values at the center points of the k finite elements are computed as

$$m_i = \mu(\mathbf{x}_i), \qquad i = 1, 2, ..., k \tag{6}$$

and stored in the mean value vector $\mathbf{m}$. The covariance between each pair of element center points is computed as

$$C_{ij} = C_{aa}(\mathbf{x}_i, \mathbf{x}_j), \qquad j = 1, 2, ..., k \tag{7}$$

and stored in the covariance matrix $\mathbf{C}$.

3 Standard Monte Carlo sampling

When the mean value vector and the covariance matrix are established, the Monte Carlo method can be employed to generate realizations that correspond to the statistics of the random field. For Gaussian random fields it is possible to generate a set of realizations with estimated statistics arbitrary close to the target statistics, and thereby to the joint distribution function, provided that a sufficiently large sample is considered. The procedure is to generate n independent Gaussian distributed random numbers with a mean of zero and a variance of one for each of the k variables. The random numbers are then stored in an $n \times k$ matrix $\mathbf{R}$. The correlation is met by performing Cholesky decomposition of the target covariance matrix $\mathbf{C}$ so that

$$\mathbf{L}\mathbf{L}^T = \mathbf{C} \tag{8}$$

where $\mathbf{L}$ is lower triangular. Then the covariance is applied as

$$\mathbf{U} = \mathbf{R}\mathbf{L}^T \tag{9}$$

yielding the $n \times k$ matrix $\mathbf{U}$ of Gaussian random numbers with a mean of zero, and a covariance in accordance with the target covariance matrix. The target mean values are applied by adding the mean value vector $\mathbf{m}$ to each row in $\mathbf{U}$.

The preservation of the Gaussian distribution from $\mathbf{R}$ to $\mathbf{U}$ is dependent on the fact that the sum of Gaussian variables is also a Gaussian variable. As other distributions are not preserved during this operation, the described procedure is only valid for Gaussian random fields. However, for non-Gaussian random fields the target covariance can be approached approximately by establishing $\mathbf{R}$ and $\mathbf{U}$ as if the field was Gaussian and then map the elements of $\mathbf{U}$ on the target distribution. This non-linear transformation is performed as

$$V_{ij} = F^{-1}\{\Phi[U_{ij}]\}, \qquad \begin{matrix} i = 1, 2, ..., n \\ j = 1, 2, ..., k \end{matrix} \tag{10}$$

where Φ represents the Gaussian cumulative distribution function, and F^{-1} represents the inverse of the target cumulative distribution function with respect to specified marginal statistics.

The transformation is illustrated in Fig. 1 and yields a sample with marginal distributions exactly approaching the target distributions, and correlation approximately approaching the target correlation. The closer the target marginal distributions are to the Gaussian distribution the better the approximation. The sampling method described above will in the following be designated SMC (Standard Monte Carlo).

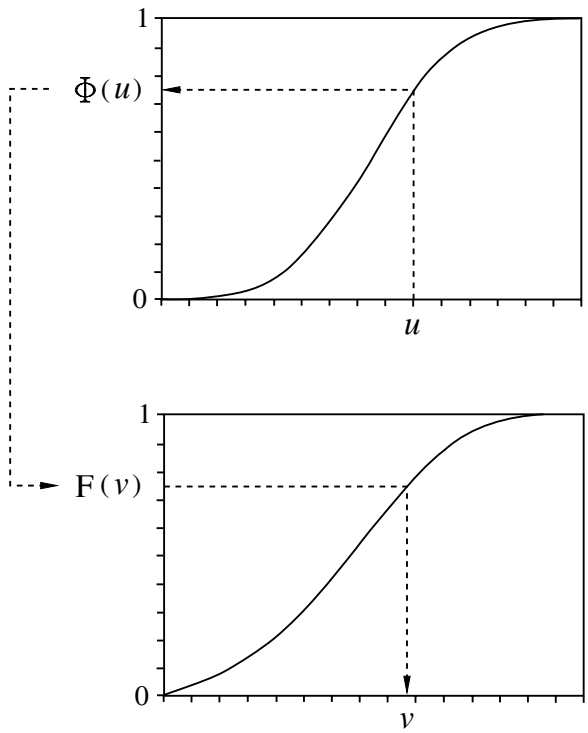

Fig. 1. *Transformation from Gaussian distribution,* $\Phi(u)$*, to non-Gaussian distribution,* $F(v)$*.*

The correlation of $\mathbf{V}$ can be improved using an iterative algorithm proposed by Yamazaki and Shinozuka (1988). Yamazaki and Shinozuka applied the algorithm on the spectral density function of the stochastic field, but also outlined the corresponding procedure for the covariance matrix decomposition method according to the following:

$\mathbf{C}_1 := \mathbf{C}$
$\mathbf{C}_2 := cov(\mathbf{V})$
repeat until $\mathbf{C}_2 \approx \mathbf{C}$
    for $i = 1 : number\ of\ variables$
        for $j = 1 : number\ of\ variables$

$$\mathbf{C}_1(i,j) := \frac{\mathbf{C}_1(i,j)}{\mathbf{C}_2(i,j)}\mathbf{C}(i,j)$$

        end
    end
    $\mathbf{L} := chol(\mathbf{C}_1)$
    $\mathbf{U} := \mathbf{R}\mathbf{L}^T$
    for $j = 1 : number\ of\ variables$
        for $i = 1 : number\ of\ realizations$

$$\mathbf{V}(i,j) := F^{-1}\{\Phi[\mathbf{U}(i,j)]\}$$

        end
    end
    $\mathbf{C}_2 := cov(\mathbf{V})$
end

where *cov* denotes estimation of the covariance, and *chol* denotes calculation of the lower triangular matrix by Cholesky decomposition. After a few iterations $\mathbf{C}_2 \approx \mathbf{C}$, and the algorithm is terminated. The sample stored in $\mathbf{V}$ then closely matches the target correlation. One problem, however, is that there are no guarantees that $\mathbf{C}_1$ remains positive definite during the iteration, not even if the midpoint method is used. If the covariance matrix is not positive definite the Cholesky decomposition can not be performed and the algorithm can not be employed.

4 Latin hypercube sampling

In order to reduce the required number of realizations, Latin hypercube sampling can be employed. This sampling scheme for computational planning was first proposed by McKay et al. (1979). As for the SMC method, the desired accuracy in the estimated distribution function determines the required number of realizations. Let n denote the required number of realizations and k the number of random variables. The sampling space is then k-dimensional. An $n \times k$ matrix $\mathbf{P}$, in which each of the k columns is a random permutation of (1,n), and an $n \times k$ matrix $\bar{\mathbf{R}}$ of independent random numbers from the uniform (0,1) distribution are established. Then the elements of the sampling matrix $\bar{\mathbf{V}}$ are determined as

$$\bar{V}_{ij} = F^{-1}\left(\frac{P_{ij} - \bar{R}_{ij}}{n}\right) \tag{11}$$

where F^{-1} represents the inverse of the target cumulative distribution function. Each row in $\bar{\mathbf{V}}$ now contains input for one deterministic computation. For two input variables and five realizations, a possible sampling plan is shown in Fig. 2. Note that the sample is spread over the entire sampling space as the generation of the Latin hypercube sampling plan requires one image from each row and each column. If n realizations from the entire sampling space had been chosen completely at random, as in SMC sampling, there is a risk that they would form a cluster and some parts of the sampling space would not be investigated.

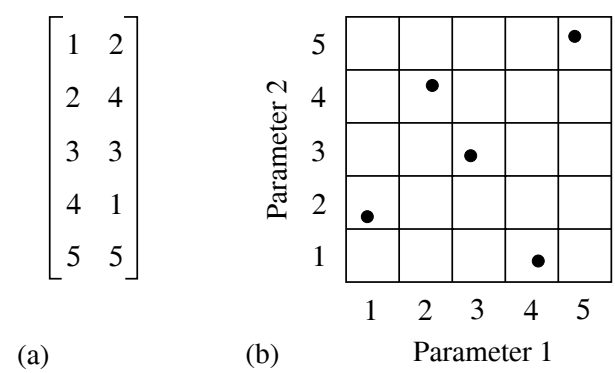

Fig. 2. *Latin cube, two variables and five realizations. The* 5×2 *matrix (a) determines the plan illustrated in (b).*

Even though the marginal distribution of each variable is efficiently represented, there is a risk that some unwanted correlation appears (Fig. 3a).

However, it has been shown (Iman and Conover 1982) that such unwanted correlation can be reduced by modifications in the permutation matrix $\mathbf{P}$. The elements of $\mathbf{P}$ are divided by the number of realizations plus one, and mapped on the (0,1) Gaussian distribution,

$$Y_{ij} = \Phi^{-1}_{(0,1)}\left(\frac{P_{ij}}{n+1}\right) \tag{12}$$

Then the covariance matrix of $\mathbf{Y}$ is estimated and Cholesky decomposed as

$$\bar{\mathbf{L}}\bar{\mathbf{L}}^T = cov(\mathbf{Y}) \tag{13}$$

where $\bar{\mathbf{L}}$ is lower triangular. A new matrix $\mathbf{Y}^*$ with sample covariance equal to the identity is computed as

$$\mathbf{Y}^* = \mathbf{Y}(\bar{\mathbf{L}}^{-1})^T \tag{14}$$

and the ranks of the elements of the columns of $\mathbf{Y}^*$ become the elements in the columns of the matrix $\mathbf{P}^*$. If the elements of $\mathbf{P}$ in Eq. (11) is replaced by the elements of this matrix, the sampling matrix $\bar{\mathbf{V}}$ will contain a considerably lower amount of unwanted correlation. Fig. 3 illustrates the effect of the correlation reduction procedure in a two variable sampling plan: (a) represents the sampling plan before, and (b) the sampling plan after the correlation reduction.

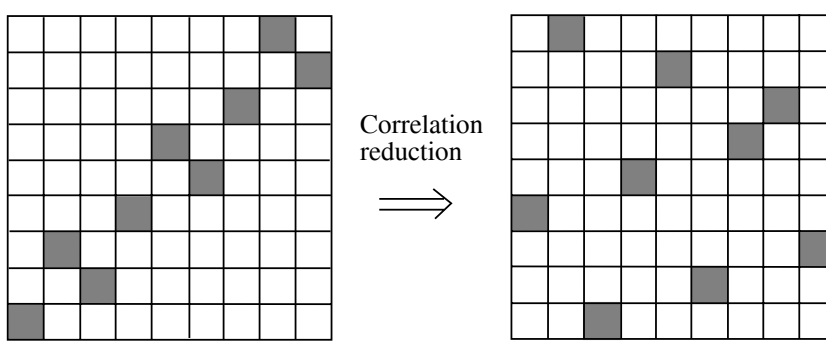

Fig. 3. *Unwanted correlation of sampling plan (a) is reduced in plan (b).*

If the target correlation matrix is different from unity the target correlation is applied by replacing Eq. (14) with

$$\mathbf{Y}^* = \mathbf{Y}(\bar{\mathbf{L}}^{-1})^T\hat{\mathbf{L}}^T \tag{15}$$

where $\hat{\mathbf{L}}$ is the lower triangular matrix from the Cholesky decomposition of the target correlation matrix. The Latin hypercube sampling method without correlation reduction will in the following be designated LHS, and the Latin hypercube sampling with correlation reduction will be designated CLHS. As for SMC sampling, the correlation of $\bar{\mathbf{V}}$ will exactly approach the target correlation if the stochastic field is Gaussian, and approximately approach the target correlation if the stochastic field is non-Gaussian. An iterative algorithm, similar to the one described in the previous section, could be employed to improve the correlation in the non-Gaussian case.

It is important to note that the correlation reduction procedure described above requires the covariance matrix of $\mathbf{Y}$ to be positive definite. This means that the inequality

$$n > k \tag{16}$$

must be fulfilled for the CLHS method. Unfortunately this is a severe restriction in many applications. If the random field is discretized to coincide with the finite element mesh, the CLHS method requires the number of realizations to be higher than the number of finite elements in the mesh. This restriction could be relieved to some extent by employing a coarser mesh for the random field, but the representation of the random field would then deteriorate, and separate discretizations of the structure and the random field would be necessary. However, if the random properties of adjacent elements are correlated, the original set of random variables can be represented by a lower number of uncorrelated random variables. This is taken advantage of in the sampling procedure proposed in the following section.

4.1 Correlation control in transformed variable space

The target covariance matrix $\mathbf{C}$ can be factorized as

$$\mathbf{D} = \mathbf{Z}^T \mathbf{C} \mathbf{Z} \tag{17}$$

where $\mathbf{D}$ is the eigenvalue matrix of $\mathbf{C}$, and $\mathbf{Z}$ is the corresponding, orthogonal eigenvector matrix. If $\mathbf{C}$ contains significant correlation, the sum of the r largest eigenvalues, where r is a small number compared to the total number of eigenvalues, is approximately equal to the trace of $\mathbf{D}$. This means that if the r largest eigenvalues are stored in the diagonal $r \times r$ matrix $\tilde{\mathbf{D}}$, and the corresponding eigenvectors are stored in the $k \times r$ matrix $\tilde{\mathbf{Z}}$ the target covariance matrix is approximately equal to

$$\tilde{\mathbf{C}} = \tilde{\mathbf{Z}} \tilde{\mathbf{D}} \tilde{\mathbf{Z}}^T \tag{18}$$

The original set of k correlated random variables, with target covariance matrix $\mathbf{C}$, can thus be replaced by a set of r uncorrelated random variables with target covariance matrix $\tilde{\mathbf{D}}$. This representation is called principal component analysis and is commonly employed in conjunction with SMC sampling to decrease the computer effort of generating random numbers. It is easy to transform the principal components, i.e. the uncorrelated random variables, back to the correlated space. Let $\tilde{\mathbf{X}}$ be an $n \times r$ matrix of Gaussian distributed random numbers with target covariance matrix $\tilde{\mathbf{D}}$. The transformation to the corresponding $n \times k$ matrix $\mathbf{X}$ with covariance matrix close to $\mathbf{C}$ is then performed as

$$\mathbf{X} = \tilde{\mathbf{X}}\tilde{\mathbf{Z}}^T \tag{19}$$

When principal component analysis is employed in conjunction with Latin hypercube sampling, with correlation reduction, it also contributes to relax the restriction of Eq. (16). The new restriction reads

$$n > r \tag{20}$$

and in many situations, as stated above, $r \ll k$. The Latin hypercube sampling on the uncorrelated variables starts by generating an $n \times r$ matrix $\tilde{\mathbf{P}}$ in which each of the r columns is a random permutation of (1,n). Then the procedure continues, equivalent to Eqs. (12–14), as

$$\tilde{Y}_{ij} = \Phi^{-1}_{(0,1)}\left(\frac{\tilde{P}_{ij}}{n+1}\right) \tag{21}$$

$$\tilde{\mathbf{L}}\tilde{\mathbf{L}}^T = cov(\tilde{\mathbf{Y}}) \tag{22}$$

$$\tilde{\mathbf{Y}}^* = \tilde{\mathbf{Y}}(\tilde{\mathbf{L}}^{-1})^T \tag{23}$$

Now the ranks of the elements of the columns of $\tilde{\mathbf{Y}}^*$ become the elements in the columns of the new matrix $\tilde{\mathbf{P}}^*$, and the final sampling matrix $\tilde{\mathbf{V}}$, in the original variable space, is established as

$$\tilde{V}_{ij} = F^{-1}\left(\Phi\left(Q_{ij}\right)\right) \tag{24}$$

where

$$\mathbf{Q} = \bar{\mathbf{Q}}\sqrt{\tilde{\mathbf{D}}}\tilde{\mathbf{Z}}^T \tag{25}$$

and

$$\bar{Q}_{ij} = \Phi^{-1}_{(0,1)} \left(\frac{\tilde{P}^*_{ij} - \tilde{R}_{ij}}{n} \right) \tag{26}$$

Note that the transformations Φ and F^{-1} are performed with respect to the specified marginal statistics of the k variables. The sampling matrix $\tilde{\mathbf{V}}$ represents the random field efficiently with respect to the marginal distributions, as well as to the correlation structure. This is confirmed by means of numerical examples presented at the end of the paper. The method will in the following be designated CTLHS (Correlation Transformed Latin Hypercube Sampling).

5 Neumann series expansion method

When the sample is determined, the deterministic solutions of the n equation systems must be computed. The system to be solved reads

$$\mathbf{K}\mathbf{u} = \mathbf{f} \tag{27}$$

where $\mathbf{K}$ is the stiffness matrix of one realization, $\mathbf{u}$ is the corresponding unknown displacement vector, and $\mathbf{f}$ is the force vector. The standard procedure is to perform a Cholesky decomposition of $\mathbf{K}$ and then solve the system by backward and forward substitutions. The major part of the computational work in this method is the Cholesky decomposition of $\mathbf{K}$ which has to be performed n times. An alternative method, proposed by Yamazaki et al. (1988), takes advantage of the similarity between the different stiffness matrices and employs the Neumann expansion technique to solve the systems. The stiffness matrix of each realization can be decomposed into two matrices,

$$\mathbf{K} = \mathbf{K}_0 + \Delta\mathbf{K} \tag{28}$$

where $\mathbf{K}_0$ is the non-fluctuating mean stiffness matrix, and $\Delta\mathbf{K}$ is the fluctuating part that is different for each realization. The displacement vector corresponding to the non-fluctuating part of the stiffness matrix can be obtained as

$$\mathbf{u}_0 = \mathbf{K}_0^{-1}\mathbf{f} \tag{29}$$

The actual inverse of the stiffness matrix is not computed, but the notation $\mathbf{K}_0^{-1}$ is used to represent a Cholesky decomposition with backward and forward

substitutions. The Neumann expansion of $\mathbf{K}^{-1}$ takes the form

$$\mathbf{K}^{-1} = (\mathbf{K}_0 + \Delta\mathbf{K})^{-1} = \left(\mathbf{I} - \mathbf{J} + \mathbf{J}^2 - \mathbf{J}^3 + \ldots\right)\mathbf{K}_0^{-1} \tag{30}$$

where $\mathbf{J} = \mathbf{K}_0^{-1}\Delta\mathbf{K}$ and $\mathbf{I}$ denotes the identity matrix. This expression for $\mathbf{K}^{-1}$ in combination with Eq. (29) result in the following series expansion for the displacement vector,

$$\mathbf{u} = \mathbf{u}_0 - \mathbf{J}\mathbf{u}_0 + \mathbf{J}^2\mathbf{u}_0 - \mathbf{J}^3\mathbf{u}_0 + \ldots \tag{31}$$

Introducing the recursive equation

$$\mathbf{u}_i = \mathbf{K}_0^{-1}\Delta\mathbf{K}\mathbf{u}_{i-1}, \qquad i = 1, 2, \ldots \tag{32}$$

the series expression of the displacement vector can be written as

$$\mathbf{u} = \mathbf{u}_0 - \mathbf{u}_1 + \mathbf{u}_2 - \mathbf{u}_3 + \ldots \tag{33}$$

The series may be truncated after a fixed number of terms, or according to an error norm as for example

$$\frac{\|\mathbf{u}_i\|_2}{\left\|\sum_{k=0}^{i}(-1)^k\mathbf{u}_k\right\|_2} \leq \varepsilon \tag{34}$$

where ε is the allowable error and $\|\mathbf{u}\|_2$ is the vector norm defined by $\sqrt{\mathbf{u}^T\mathbf{u}}$. The major advantage of the Neumann series expansion method is that only the non-fluctuating part of the stiffness matrix has to be factorized and this only once. The additional computational work consists of elementary matrix-vector multiplications and additions of matrices. Thus a considerable amount of computational resources can be saved by using this method. However, it must be checked that the series of each realization converges. This can be done by the error norm given by Eq. (34) in combination with a maximum number of terms, or by concluding that the series does not converge when

$$\|\mathbf{u}_i\|_2 \leq \|\mathbf{u}_{i+1}\|_2 \tag{35}$$

Yamazaki et al. (1988) showed that the convergence criterion of Eq. (34) can always be met by replacing the decomposition of Eq. (28) by

$$\mathbf{K} = m\mathbf{K}_0 + \Delta\mathbf{K}^* \tag{36}$$

where m is a scalar chosen to satisfy the convergence criterion. It is beyond the scope of the present paper to describe this modified procedure in detail, but it should be noted that in order to compute the value of the scalar m it is necessary to compute the eigenvalue of $\mathbf{J}$ having the largest absolute value. Unfortunately, the calculations required to find that eigenvalue appear to be more demanding, in terms of computational resources, than to perform the Cholesky decomposition of $\mathbf{K}$. Therefore, the Neumann series expansion method should only be employed for applications where most of the realizations result in series that are convergent without modifications. If a small number of the realizations result in non-convergent series, the equation systems of these can be solved by the standard Cholesky decomposition method.

6 Taylor series expansion method

In this method, the unknown random field is approximated by a Taylor series expansion. The statistics of the random field are computed by integrating the product of this series expansion and the probability distribution of the input variables over the domain of these variables. An extensive description of the method is found in Kleiber and Hien (1992).

The stiffness relation of the structure reads

$$K_{\alpha\beta}u_\beta = f_\alpha \tag{37}$$

where $K_{\alpha\beta}$ and f_α are the stiffness matrix and force vector, respectively, and u_β represents the unknown random displacement field of the system. A Taylor series expansion of the displacement vector is established as

$$u_\alpha(s_\varrho) = u_\alpha^0(s_\varrho^0) + u_\alpha^{,\rho}(s_\varrho^0)\Delta s_\rho + \frac{1}{2}u_\alpha^{,\rho\sigma}(s_\varrho^0)\Delta s_\rho \Delta s_\sigma + \cdots \tag{38}$$

where $u_\alpha^0(s_\varrho^0)$ is the deterministic solution of the system corresponding to the mean values of the stochastic input variables, and $u_\alpha^{,\rho}(s_\varrho^0)$ and $u_\alpha^{,\rho\sigma}(s_\varrho^0)$ are the first and second derivatives of the displacement vector with respect to the stochastic input variables. The mean value vector and the covariance matrix of the displacements are defined as

$$E[u_\alpha] = \int_{-\infty}^{\infty}\int_{-\infty}^{\infty}\cdots\int_{-\infty}^{\infty} u_\alpha p_k(s_1, s_2, \ldots, s_k) ds_1 ds_2 \ldots ds_k \tag{39}$$

$$cov[u_\alpha, u_\beta] = \int_{-\infty}^{\infty}\int_{-\infty}^{\infty}\cdots\int_{-\infty}^{\infty}\{u_\alpha - E[u_\alpha]\}\{u_\beta - E[u_\beta]\}$$
$$p_k(s_1, s_2, \ldots, s_k)ds_1 ds_2 \ldots ds_k \tag{40}$$

where p_k is the k-dimensional probability density function of the stochastic input variables and k is the number of stochastic input variables of the system. Substituting Eq. (38) into Eqs. (39–40), disregarding higher order moments than the second order, yields

$$E[u_\alpha] = u_\alpha^0 + \frac{1}{2}u_\alpha^{,\rho\sigma}C_s^{\rho\sigma} \tag{41}$$

$$cov[u_\alpha, u_\beta] = u_\alpha^{,\rho}u_\beta^{,\sigma}C_s^{\rho\sigma} \tag{42}$$

where $C_s^{\rho\sigma}$ is the covariance matrix of the stochastic input variables. The derivatives of the displacements are obtained by partial derivatives of the system equation. The first and second order partial derivatives read

$$K_{\alpha\beta}^0(s_\varrho^0)u_\beta^{,\rho}(s_\varrho^0) = f_\alpha^{,\rho}(s_\varrho^0) - K_{\alpha\beta}^{,\rho}u_\beta^0(s_\varrho^0) \tag{43}$$

$$K_{\alpha\beta}^0(s_\varrho^0)u_\beta^{,\rho\sigma}(s_\varrho^0) = f_\alpha^{,\rho\sigma}(s_\varrho^0) - 2K_{\alpha\beta}^{,\rho}(s_\varrho^0)u_\beta^{,\sigma}(s_\varrho^0) - K_{\alpha\beta}^{,\rho\sigma}(s_\varrho^0)u_\beta^0(s_\varrho^0) \tag{44}$$

When the derivatives of the displacement vector are derived, they are substituted into Eqs. (41–42) and the displacement statistics are computed. The described procedure shows the basic concept of the Taylor series expansion method. When the statistics of the displacements are computed, the statistics of secondary unknowns, such as strains and stresses, can be derived. This procedure, however, is not dealt with herein.

As in the sampling methods, the original set of stochastic input variables can be replaced by a set of uncorrelated stochastic input variables, i.e. principal components. The transformation of the covariance matrix is performed as

$$D_t^{\check{\rho}\check{\sigma}} = Z_{\check{\rho}\sigma}C_s^{\rho\sigma}Z_{\rho\check{\sigma}} \tag{45}$$

where $D_t^{\check{\rho}\check{\sigma}}$ is the diagonal covariance matrix of the new set of random variables, t, and $Z_{\check{\rho}\sigma}$ contains the eigenvectors of $C_s^{\rho\sigma}$ corresponding to the $\check{k}$ largest eigenvalues of $C_s^{\rho\sigma}$. The expressions for the displacement statistics become

$$E[u_\alpha] = u_\alpha^0 + \frac{1}{2}u_\alpha^{,\check{\rho}\check{\sigma}}D_t^{\check{\rho}\check{\sigma}} \tag{46}$$

$$cov[u_\alpha, u_\beta] = u_\alpha^{,\check{\rho}}u_\beta^{,\check{\sigma}}D_t^{\check{\rho}\check{\sigma}} \tag{47}$$

where the displacement derivatives are derived from the partial derivatives of the system equation

$$K^0_{\alpha\beta}(t^0_{\check{\varrho}})u^{,\check{\rho}}_{\beta}(t^0_{\check{\varrho}}) = f^{,\check{\rho}}_{\alpha}(t^0_{\check{\varrho}}) - K^{,\check{\rho}}_{\alpha\beta}(t^0_{\check{\varrho}})u^0_{\beta}(t^0_{\check{\varrho}}) \tag{48}$$

$$K^0_{\alpha\beta}(t^0_{\check{\varrho}})u^{,\check{\rho}\check{\sigma}}_{\beta}(t^0_{\check{\varrho}}) = f^{,\check{\rho}\check{\sigma}}_{\alpha}(t^0_{\check{\varrho}}) - 2K^{,\check{\rho}}_{\alpha\beta}(t^0_{\check{\varrho}})u^{,\check{\sigma}}_{\beta}(t^0_{\check{\varrho}}) - K^{,\check{\rho}\check{\sigma}}_{\alpha\beta}(t^0_{\check{\varrho}})u^0_{\beta}(t^0_{\check{\varrho}}) \tag{49}$$

The derivatives of the system matrix are computed as

$$K^{,\check{\rho}}_{\alpha\beta}(t^0_{\check{\varrho}}) = Z_{\check{\rho}\rho}K^{\rho}_{\alpha\beta}(s^0_{\varrho}) \tag{50}$$

$$K^{,\check{\rho}\check{\sigma}}_{\alpha\beta}(t^0_{\check{\varrho}}) = Z_{\check{\rho}\sigma}K^{,\rho\sigma}_{\alpha\beta}(s^0_{\varrho})Z_{\rho\check{\sigma}} \tag{51}$$

It should be emphasized, however, that as $D^{\check{\rho}\check{\sigma}}_t$ is diagonal, only the subset with index $\check{\rho} = \check{\sigma}$ has to be dealt with in Eqs. (46–51). Thus no mixed derivatives of the system matrix with respect to the transformed set of random variables have to be derived. This advantage, and the fact that the considered number of principal components is much lower than the original number of random variables, are the reasons why the method with transformation often can be employed at a considerably lower computational cost than the method without transformation. A disadvantage of the principal component approach is that the extremely sparse structure of the third order tensor $K^{,\rho}_{\alpha\beta}(s^0_{\varrho})$ is damaged when transformed according to Eq. (50).

7 Numerical example

To compare the accuracy and efficiency of the described methods, and to a certain degree illustrate the significance of the random field discretization, a numerical example is employed. All calculations are performed on a SGI Octane, 195 MHz computer, using the software MATLAB (*MATLAB* 1999). A square plate with unit side length and unit thickness is modeled by plane-stress Melosh elements. The material of the plate is assumed to be isotropic with stochastic Young's modulus and deterministic Poisson's ratio, $\nu = 0.3$. The plate is loaded with a deterministic, uniformly distributed load of unit magnitude. Nodal displacements in the y-direction are constrained along the lower edge, and nodal displacements in both directions are constrained at the lower left corner. Fig. 4 shows the geometry, loading, and boundary conditions of the structure. Note that in the deterministic case, with constant Young's modulus in the entire plate, the displacement field is computed exactly independently of the finite element mesh. Thus the need of a refined mesh is solely to capture the properties of the random field, i.e. the stochastic Young's modulus. A similar example was used by Yamazaki et al. (1988) to illustrate

the advantages of using the Neumann series expansion method in conjunction with SMC simulations.

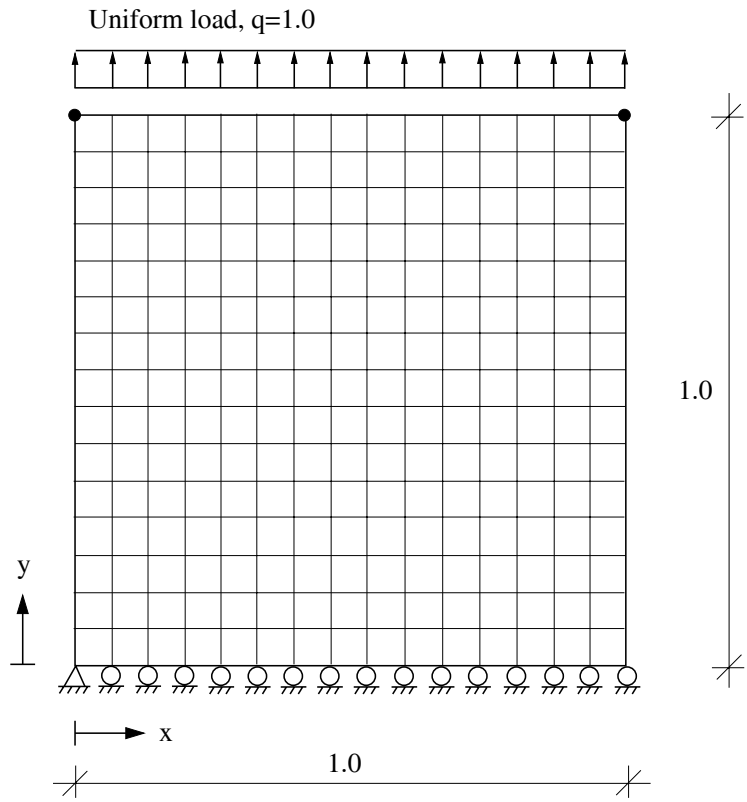

Fig. 4. *Square plate, loaded in tension, modeled by* 15×15 *elements.*

7.1 Correlation and discretization

A log-normal random field is adopted for the Young's modulus of the plate. The field is characterized by its mean value function, which is constant and equal to one in the entire plate, and the isotropic auto-covariance function,

$$C_{ij} = \sigma_0^2 \; exp\left[- \left(\frac{|\xi_{ij}|}{d} \right)^2 \right] \tag{52}$$

in which σ_0 is the standard deviation of the random field, and d is a positive parameter such that a larger value indicates a stronger correlation. The random field is discretized using the midpoint method. Thus $|\xi_{ij}|$ is the distance

between the centroid of element i and the centroid of element j, and the size of the covariance matrix $\mathbf{C}$ is equal to the square of the number of elements in the plate. Fig. 5 shows the correlation according to Eq. (52) as a function of the distance, and the discretization of the correlation function corresponding to the midpoint method with 15 elements along the edge of the plate. It is quite clear from Fig. 5 that the discretization yields better approximations of the correlation function for large values of d.

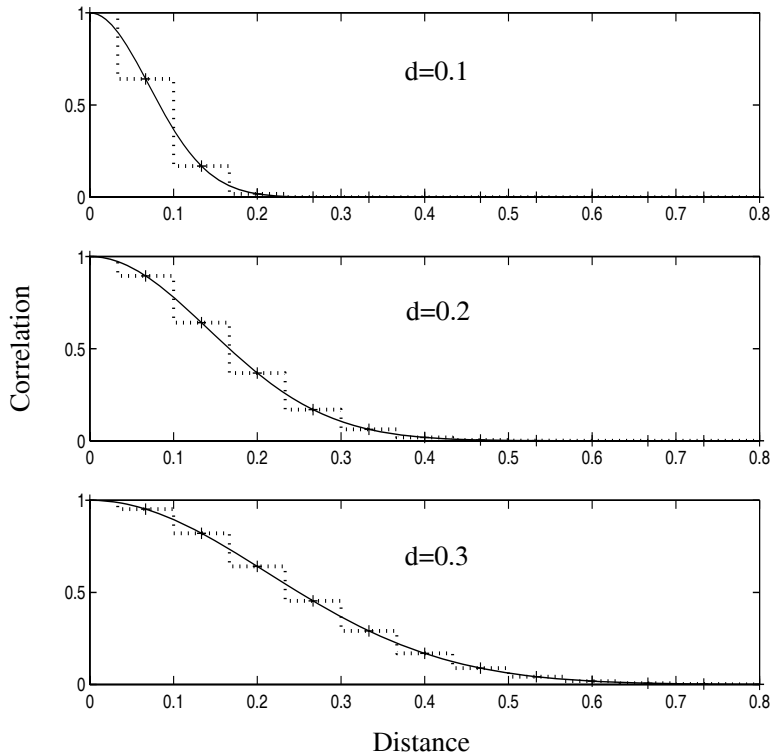

Fig. 5. *Correlation as function of distance.*

The displacement field of the plate is now evaluated for all combinations of $d = 0.1, 0.2, 0.3$ and $\sigma_0 = 0.1, 0.2, 0.3$ in order to investigate how fine the finite element mesh has to be to capture the random field sufficiently well. Calculations are performed using 10, 15, 20, and 25 elements along the edge of the plate. The Latin hypercube methods are employed, as they are more efficient than the SMC method in obtaining the statistics of the displacement field. A sample of 10,000 realizations is established for each calculation. The CLHS is used when possible, but in the models with fine mesh and strong correlation the correlation matrix becomes close to singular, resulting in numerical difficulties. In those cases the CTLHS is employed, considering a sufficiently large number of the eigenvalues of the covariance matrix. The quantities given in Table 1 are the mean value of the vertical displacement of the upper right

corner of the plate, the variance of the same displacement, and the covariance between the vertical displacements of the upper left and upper right corners. An asterisk in Table 1 indicates that the CTLHS is used for that calculation. The significance of the values in Table 1 is not evaluated in the strict mathematical sense but five repetitive simulations of each model are performed showing that the errors should not exceed one unit of the last digit given of each value.

Fig. 5 illustrates that the same finite element mesh represents a different quality of the correlation function discretization depending on the value of the parameter d; the higher the value of d the better the representation. Thus a short correlation distance requires a finer mesh than a longer correlation distance. This is confirmed by the values in Table 1. In the following study of the performance of the different sampling methods and expansion methods, the correlation of the Young's modulus is determined by $d = 0.2$, and the 15×15 element mesh is employed.

7.2 Comparison of different methods

The efficiency of the different sampling methods is first and foremost dependent on the accuracy of the output distributions and statistics that can be achieved for a given number of realizations. The computer effort of generating the input sample is in most finite element applications comparatively low. As a measure of the ability of capturing the true values of the statistics the coefficient of variation, R, of the statistics is employed. A good performance of the applied sampling method results in a low coefficient of variation of the estimated output statistics. Naturally, also the bias due to the different sampling methods should be evaluated. A brief investigation on this matter is performed, though not thoroughly accounted for herein, showing that no significant bias appears in the evaluated statistics. However, it should be noted, that in some situations significant bias actually appears for the Latin hypercube methods with correlation control. This has been illustrated by Kjell (1995).

The coefficient of variation of the statistics is evaluated for each combination of $\sigma_0 = 0.1$, 0.2, 0.3, and $n = 10$, 100, 1000. One hundred calculations for each combination are performed in order to estimate the coefficient of variation of the statistics. The expression reads

$$R(\triangle) = \frac{\sqrt{\sum_{i=1}^{100} (\triangle_i - \triangle_{mean})^2 / 99}}{\triangle_{mean}} \tag{53}$$

Standard deviation and element mesh		Mean value of vertical displacement			Variance of vertical displacement			Covariance of vertical displacements		
		$d = 0.1$	$d = 0.2$	$d = 0.3$	$d = 0.1$	$d = 0.2$	$d = 0.3$	$d = 0.1$	$d = 0.2$	$d = 0.3$
$\sigma_0 = 0.1$	10×10	1.00697	1.00807	1.00870	0.00120	0.00318	0.00519	-0.000350	-0.00099	-0.00147
	15×15	1.00721	1.00813	1.00873*	0.00116	0.00315	0.00515*	-0.000343	-0.00098	-0.00148*
	20×20	1.00735	1.00816*	1.00873*	0.00115	0.00313*	0.00514*	-0.000341	-0.00098*	-0.00148*
	25×25	1.00742	1.00818*	1.00874*	0.00114	0.00312*	0.00513*	-0.000340	-0.00098*	-0.00148*
$\sigma_0 = 0.2$	10×10	1.02776	1.03216	1.03474	0.00496	0.0132	0.0216	-0.00143	-0.00406	-0.0061
	15×15	1.02873	1.03243	1.03482*	0.00480	0.0131	0.0215*	-0.00141	-0.00404	-0.0061*
	20×20	1.02927	1.03255*	1.03487*	0.00474	0.0130*	0.0214*	-0.00140	-0.00403*	-0.0061*
	25×25	1.02955	1.03261*	1.03487*	0.00472	0.0130*	0.0214*	-0.00140	-0.00403*	-0.0061*
$\sigma_0 = 0.3$	10×10	1.0620	1.0720	1.0779	0.0117	0.0315	0.0519	-0.00334	-0.0096	-0.0144
	15×15	1.0642	1.0726	1.0781*	0.0114	0.0312	0.0516*	-0.00329	-0.0095	-0.0144*
	20×20	1.0654	1.0729*	1.0782*	0.0112	0.0311*	0.0515*	-0.00329	-0.0095*	-0.0144*
	25×25	1.0660	1.0730*	1.0782*	0.0112	0.0310*	0.0515*	-0.00327	-0.0095*	-0.0144*

Table 1. *Statistics of vertical displacement of upper corners. CTLHS indicated by* $*$.

where

$$\triangle_{mean} = \sum_{i=1}^{100} \triangle_i / 100 \tag{54}$$

and $\triangle$ represents the mean value, the variance, or the covariance. Actually, for the results presented in Table 2, 5×100 calculations are performed in order to verify the significance of the computed numbers. The relative error received using the Taylor series expansion method is also given in Table 2. Even though this error is not equivalent to the coefficient of variation given for the sampling methods it can be used for a comparison of the different strategies.

Consider first the coefficient of variation of the mean value. It is quite clear that all the Latin hypercube methods perform excellently, at least ten times better than the SMC method. When applicable, the CLHS is the most efficient method but as it requires n to be higher than the number of stochastic variables, in the present case 15×15, it can not be used for $n = 10$, or $n = 100$. The CTLHS is suitable when the $n-1$ largest eigenvalues are sufficient to represent the random field, and for $n = 100$, more than 99.99% of the eigenvalue sum is captured. The performance of the Taylor series expansion method is excellent when $\sigma_0 = 0.1$, but even for $\sigma_0 = 0.3$ the error is smaller than the coefficient of variation using any of the sampling methods with $n = 100$.

More interesting than the mean displacements is the ability to capture the variance and the correlation of the displacements as they normally require much larger samples. For example, using the SMC method with $n = 10$, and $\sigma_0 = 0.1$, the coefficient of variation of the variance amounts to 50% whereas the coefficient of variation of the mean value only amounts to 2%. Table 2 shows that the LHS is only slightly better than the SMC method, whereas the CLHS and the CTLHS are much more efficient. For example, using the CTLHS with $n = 100$, better results are achieved regarding the variance and correlation than using the LHS with $n = 1000$. Note that the CTLHS is almost as efficient as the CLHS. Furthermore, a comparison shows that the Taylor series expansion method performs approximately as well as the CTLHS with $n = 100$. The performance of the Taylor series expansion method is relatively better for small values of σ_0.

As a principal component representation is employed for the CTLHS, and can be employed for the Taylor series expansion method, the number of eigenvalues required for the analysis should be studied. Fig. 6 shows, for $d = 0.1$, 0.2, 0.3, the relative error of the mean value and the relative error of the variance as functions of the number of eigenvalues considered. It is clear that the required number of eigenvalues decreases as the correlation of the random field increases.

Standard deviation and sampling method		Coefficient of variation of the mean value, $R(mean)$			Coefficient of variation of the variance, $R(var)$			Coefficient of variation of the covariance, $R(cov)$		
		$n = 10$	100	1000	$n = 10$	100	1000	$n = 10$	100	1000
$\sigma_0 = 0.1$	SMC	0.018	0.005	0.0019	0.5	0.14	0.05	1.1	0.3	0.11
	LHS	0.0012	0.00016	0.00005	0.4	0.12	0.04	1.1	0.3	0.10
	CLHS	–	–	0.000008	–	–	0.004	–	–	0.008
	CTLHS	–	0.0003	0.00002	–	0.03	0.005	–	0.06	0.010
	Taylor	0.00001			0.01			0.01		
$\sigma_0 = 0.2$	SMC	0.04	0.011	0.004	0.5	0.14	0.05	1.1	0.3	0.11
	LHS	0.0028	0.0006	0.00019	0.4	0.12	0.04	1.0	0.3	0.11
	CLHS	–	–	0.00004	–	–	0.008	–	–	0.019
	CTLHS	–	0.0006	0.00006	–	0.03	0.009	–	0.07	0.018
	Taylor	0.0002			0.05			0.03		
$\sigma_0 = 0.3$	SMC	0.05	0.016	0.006	0.5	0.15	0.05	1.2	0.3	0.11
	LHS	0.006	0.0013	0.0004	0.4	0.12	0.04	1.1	0.3	0.11
	CLHS	–	–	0.00008	–	–	0.010	–	–	0.02
	CTLHS	–	0.0009	0.00013	–	0.05	0.013	–	0.09	0.02
	Taylor	0.0006			0.10			0.08		

Table 2. *Coefficient of variation of statistics using different sampling methods, and relative error using the Taylor series expansion method.*

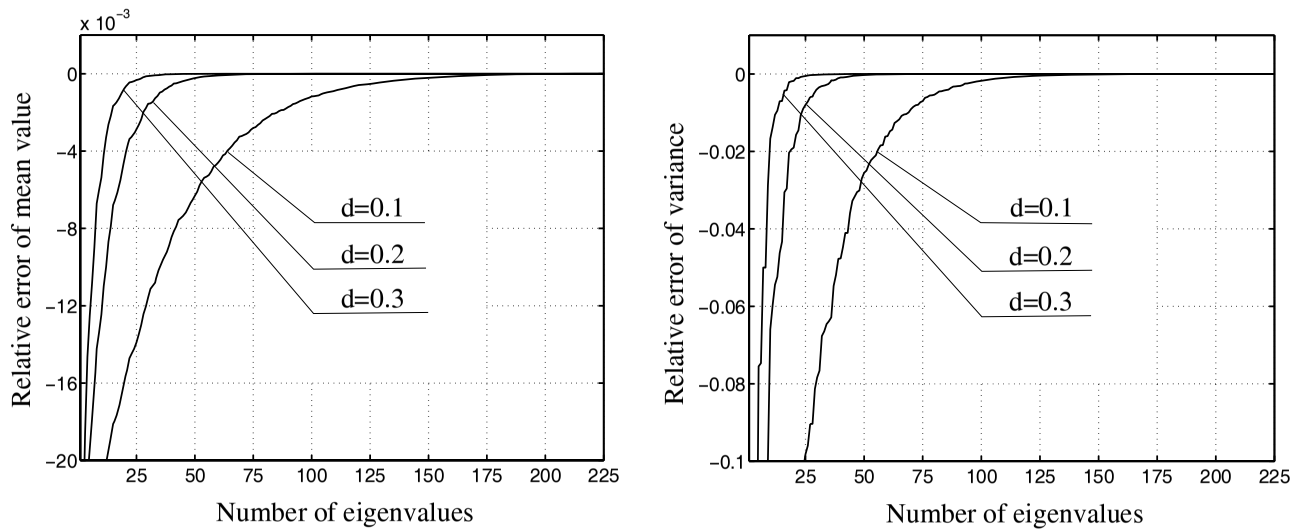

Fig. 6. *Relative error as a function of the number of eigenvalues.*

As pointed out earlier, the sampling methods can be employed in conjunction with the Neumann series expansion method in order to reduce the computational effort required for analyzing each realization. Realizations that, according to Eq. (35), do not result in a convergent series are solved with the standard Cholesky decomposition method. If the standard deviation of the random field is small, the number of such realizations is quite low compared to n, but they are important to detect as they otherwise would significantly affect the statistics of the displacement field. Table 3 shows the error of the displacement statistics, the same as in the previous tables, due to the approximation of the Neumann series expansion. The number of realizations treated with the standard Cholesky decomposition is given in parenthesis. The values of Table 3 are evaluated using the CLHS with $n = 1000$, and $d = 0.2$, but it should be noted that the errors given are due to the Neumann expansion and would not decrease or increase if another number of realizations was considered or if any of the other sampling methods was employed instead of the CLHS.

Fig. 7 shows how the solution of the Neumann series expansion method approaches the solution of the Cholesky decomposition method as the order of the expansion increases. The relative errors of the mean displacement and the variance of the displacement of the upper right corner are given as functions of the order of the Neumann series expansion for $d = \sigma_0 = 0.2$. It is noted that the error of the mean displacement according to the second order expansion, and the error of the variance of the displacement according to the first order expansion are comparable to the corresponding errors when the Taylor series expansion method is employed.

To compare the Neumann series expansion method with the Cholesky decomposition method, and the sampling methods with the Taylor series expansion method, the computational effort required for the different methods must be evaluated. However, it is not an easy task to perform a fair comparison as the required computational effort very much depends on the implementation in the computer code. Therefore, it should be noted that even though much effort is spent on implementing the different methods efficiently, the relations between the CPU–times given in Tables 4–6 could be quite different if the calculations were performed using another computer code. Nevertheless, Table 4 shows that the Neumann series expansion method can be employed at a considerably lower cost than the standard Cholesky method, and the difference is more pronounced for large systems. Table 5 shows the CPU–times required for generating one log-normal realization using the different sampling methods. The values given are valid for $n = 100$ and $n = 1000$, the latter in parenthesis. For small values of n, the major part of the cost is due to initial preparation of the sampling such as Cholesky decomposition or eigenvalue transformation of the covariance matrix. Considering the total computational costs of generating the sample and solving the corresponding equation systems, it appears

statistics		2nd order		4th order		6th order		8th order	
mean	$\sigma_0 = 0.1$	0.000006	(0)	0.000009	(0)	0.0000010	(0)	0.00000012	(0)
value,	$\sigma_0 = 0.2$	0.00010	(6)	0.0005	(24)	0.0003	(39)	0.00015	(53)
	$\sigma_0 = 0.3$	0.0003	(219)	0.003	(704)	0.002	(1107)	0.0012	(1424)
variance,	$\sigma_0 = 0.1$	0.05	(0)	0.002	(0)	0.00013	(0)	0.000011	(0)
	$\sigma_0 = 0.2$	0.17	(6)	0.03	(24)	0.009	(39)	0.005	(53)
	$\sigma_0 = 0.3$	0.3	(219)	0.10	(704)	0.04	(1107)	0.02	(1424)
covar-	$\sigma_0 = 0.1$	0.04	(0)	0.0017	(0)	0.00010	(0)	0.000009	(0)
iance,	$\sigma_0 = 0.2$	0.16	(6)	0.03	(24)	0.009	(39)	0.005	(53)
	$\sigma_0 = 0.3$	0.3	(219)	0.10	(704)	0.04	(1107)	0.02	(1424)

Table 3. *Error of displacement statistics due to approximation of Neumann series expansion.*

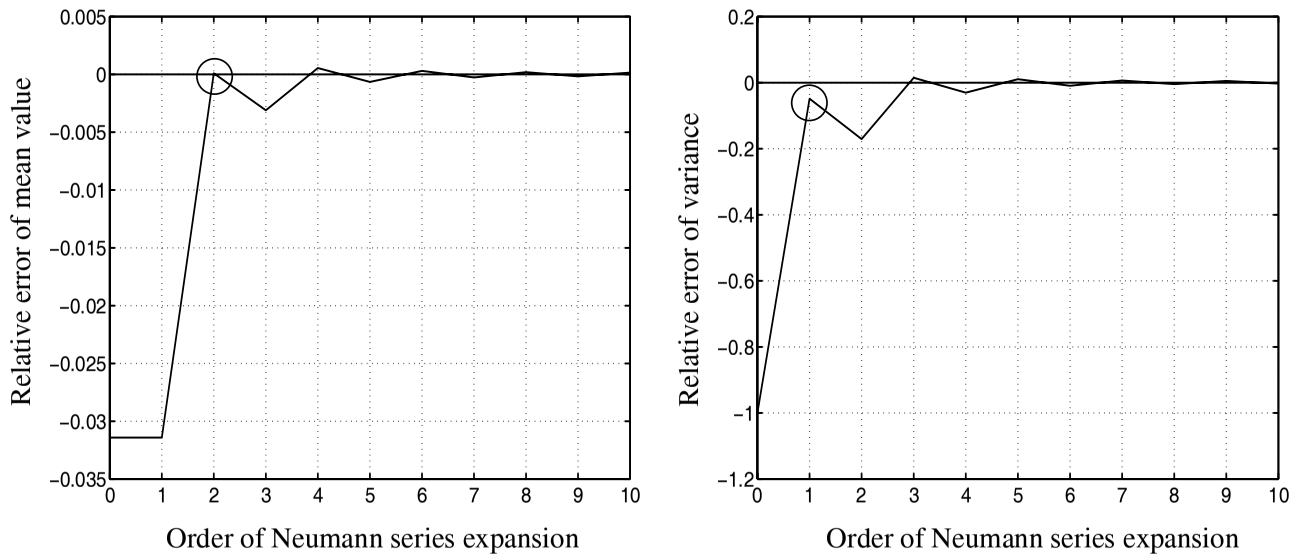

Fig. 7. *Relative error as a function of the order of the Neumann series expansion.*

most favorable to employ the CTLHS in conjunction with the Neumann series expansion method.

Table 6 shows the CPU–times required using the Taylor series expansion method with and without eigenvalue transformation. The displayed CPU–times for the latter alternative correspond to 100 considered eigenvalues. For small problems the values of Table 6 indicate that the eigenvalue transformation method is better only if the considered number of eigenvalues is much smaller than the number of original random variables. A comparison between the Taylor series expansion method and the CTLHS method in conjunction with the Neumann series expansion method is hard to perform as the types of error of the two approaches are different, and as the implementation might favor one of the approaches before the other. Nevertheless, the square plate example shows that in a case with $\sigma_0 = 0.2$, the quality of the computed statistics is approximately the same when the CTLHS, in conjunction with the Neumann series expansion method (6th order), is employed and when the Taylor series expansion method is employed. The computational cost, however, is almost twice as high using the latter approach.

element mesh	Cholesky	N. 2nd ord.	N. 4th ord.	N. 6th ord.	N. 8th ord.
15×15	0.047	0.022	0.036	0.050	0.064
25×25	0.241	0.077	0.130	0.184	0.238
50×50	2.430	0.441	0.787	1.137	1.506

Table 4. *CPU-time required for the Cholesky and Neumann methods.*

element mesh	SMC	LHS	CLHS	CTLHS*
15×15	0.008 (0.009)	0.014 (0.018)	– (0.018)	0.023 (0.018)
25×25	0.036 (0.028)	0.055 (0.051)	– (0.059)	0.282 (0.060)
50×50	1.116 (0.227)	1.255 (0.330)	– –	1.876 (0.346)

Table 5. *CPU-time required for generating input samples.* * *One hundred eigenvalues considered.*

element mesh	No transf.	eig.transf.*
15×15	1.65	14.83
25×25	16.3	74.0
50×50	558	551

Table 6. *CPU-time required for the Taylor series expansion method.* * *One hundred eigenvalues considered.*

8 Conclusions

The main objective of this paper is to introduce the correlation controlled Latin hypercube sampling plan in transformed variable space for finite element applications. As the sampling plan is only used to establish input data for a number of deterministic runs, the method can be unimpededly employed for applications involving complicated mechanical processes such as geometrical and material non-linearities, and dynamics. Existing finite element codes, developed for deterministic analysis, can without modifications be employed in conjunction with the sampling method.

The paper shows the superior efficiency of the suggested method compared to standard Monte Carlo sampling and Latin hypercube sampling without correlation control. It also shows the superior applicability of the method compared to correlation controlled Latin hypercube sampling in original variable space.

The Neumann series expansion method, used by several researchers in conjunction with standard Monte Carlo sampling, can also be combined with the proposed method. This combination is the most efficient approach of the alternatives presented. It appears to be even more efficient than the Taylor series expansion method which is a method with significant limitations in general applicability, and availability for everyday engineering design practice.

9 References

Chakraborty, S., and Dey, S. S. (1996), "Stochastic finite element simulation of random structure on uncertain foundation under random loading." *Int. J. Mech. Sci.*, 38(11), 1209–1218.

Harris, C. M., Hoffman, K. L., and Yarrow, L.-A. (1995), "Obtaining minimum-correlation Latin hypercube sampling plans using IP-based heuristic." *OR Spectrum*, 17, 139–148.

Iman, R. L., and Conover, W. J. (1982), "A distribution-free approach to inducing rank correlation among input variables." *Communications in Statistics - Simulation and Computation*, 11(3), 311–334.

Kjell G. (1995), "Computer experiments with application to earthquake engineering." *Rep. 1995:7, Studies in Statistical Quality Control and Reliability,* Chalmers Univ. of Techn., Dep. of Math. Stat., Gothenburg, Sweden.

Kleiber, M., and Hien, T. D. (1992), "The stochastic finite element method." *Wiley*, Chichester, England.

Lawrence, M. A. (1987), "Basis random variables in finite element analysis."

Int. J. Num. Meth. Engrg., 24, 1849–1863.

Liu, W. K., Belytschko, T., and Mani, A. (1986), "Random field finite elements." *Int. J. Num. Meth. Engrg.*, 23, 1831–1845.

MATLAB. (1999), "High-performance numerical computation and visualization software." *Version 5.3, The Math Works Inc*, Natic Ma.

Matthies, H. G., Brenner, C. E., Bucher, C. G., and Soares, C. G. (1997) "Uncertainties in probabilistic numerical analysis of structures and solids – stochastic finite elements." *Structural Safety*, 19(3), 283–336.

McKay, M. D., Conover, W. J., and Beckman R. J. (1979), "A comparison of three methods for selecting values of input variables in the analysis of output from a computer code." *Technometrics*, 21(2), 239–245.

Owen, A. B. (1994), "Controlling correlations in Latin hypercube samples." *J. American Stat. Ass.*, 89(428), 1517–1522.

Papadrakakis, M., and Papadopoulos, V. (1996), "Robust and efficient methods for stochastic finite element analysis using Monte Carlo simulation." *Comput. Methods Appl. Mech. Engrg.*, 134, 325–340.

Sandberg, G., Kjell, G., and de Maré, J. (1997), "Computational planning using Latin hypercube sampling." *Report TVSM–7118*, Lund Inst. of Techn., Div. of Struct. Mech., Lund, Sweden.

Sandberg, G., and Olsson, A. (1999), "Failure sensitivity analysis of engineering structures." *Computers and Structures*, 72, 525–534.

Shinozuka, M., and Deodatis, G. (1988), "Response variability of stochastic finite element systems." *J. Engrg. Mech.*, ASCE, 114(3), 499–519.

Spanos, P. D. and Ghanem, R. (1989), "Stochastic finite element expansion for random media." *J. Engrg. Mech.*, ASCE, 115(5), 1035–1053.

Stein, M. (1987), "Large sample properties of simulations using Latin hypercube sampling." *Technometrics*, 29(2), 143–151.

Vanmarcke, E. (1984), "Random fields." *MIT Press*, Cambridge, Mass.

Yamazaki, F., Shinozuka, M., and Dasgupta, G. (1988), "Neumann expansion for stochastic finite element analysis." *J. Engrg. Mech.*, ASCE, 114(8), 1335–1354.

Yamazaki, F., and Shinozuka, M. (1988), "Digital generation of non-Gaussian stochastic fields." *J. Engrg. Mech.*, ASCE, 114(7), 1383–1397.